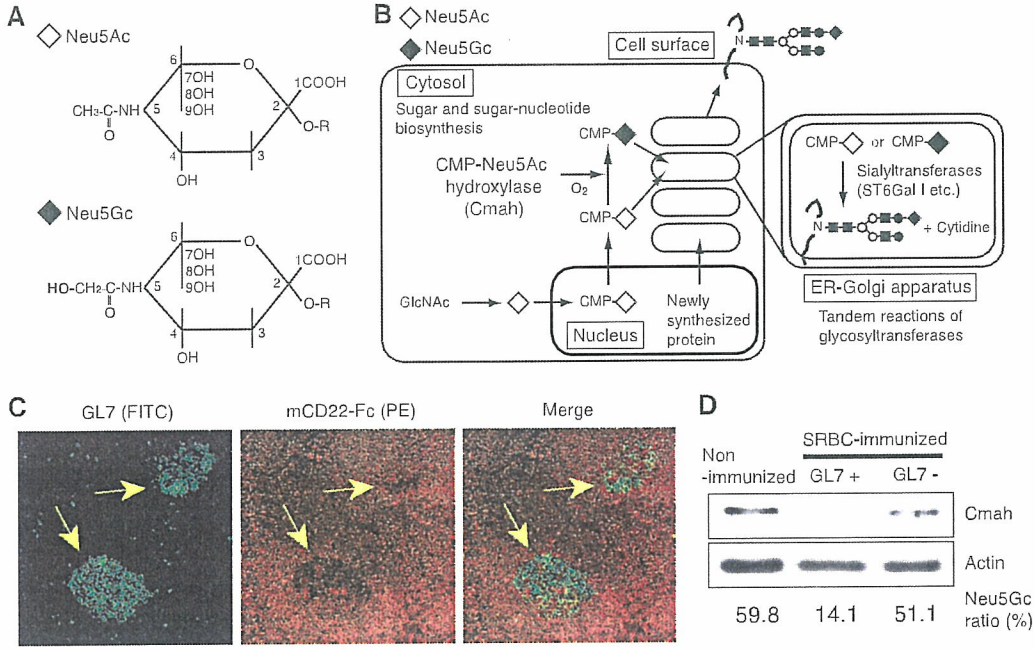

FIG. 3. Change in Sia species in germinal centers. (A) Structural differences between two major molecular species of Sia. The metabolic precursor Neu5Ac and its modified form Neu5Gc differ only by an oxygen atom at the C-5 position. The conversion of CMP-Neu5Ac to CMP-Neu5Gc is catalyzed by the enzyme Cmah. (B) Biosynthesis of sialylated glycoproteins destined for the cell surface. Cytosolic metabolism of Sia is responsible for the abundance of the molecular species of Sia on the cell surface, as a given ratio of cytosolic CMP-Sia is imported into the Golgi apparatus and then used by the sialyltransferases for the biosynthesis of glycoproteins en route to the plasma membrane. (C) Loss of CD22 ligand in germinal centers. Spleen sections of SRBC-immunized mice (10 days after immunization) were costained with FITC-conjugated GL7 and mCD22-Fc precomplexed with R-PE-conjugated anti-human IgG. The mCD22-Fc is a chimeric probe that binds to the CD22 ligand. Arrows indicate germinal centers. (D) Downregulation of Cmah expression in germinal center B cells. GL7-positive germinal center cells and GL7-negative cells were prepared from a B-cell-enriched fraction derived from the spleen of a mouse 12 days after immunization with SRBC. Ultracentrifugation supernatant fractions (cytosolic fractions) of untreated mouse B cells (nonimmunized; control), GL7-positive B cells (GL7+), and GL7-negative B cells (GL7−) were subjected to immunoblotting with anti-mouse Cmah antibody and antiactin antibody (to demonstrate equal loading of samples). The Neu5Gc/(Neu5Ac+Neu5Gc) ratio of the ultracentrifugation pellets (membrane fractions) of each cell type was measured by HPLC.

LPS-stimulated B blasts (Fig. 4C), further confirming the responsibility of *Cmah* for the repression of the appearance of the GL7 epitope. After 48 h of stimulation with LPS, *Gapdh* expression increased by about 30% (Fig. 4A). This may be attributable to the blastic transformation of LPS-stimulated proliferating B cells (B blasts), which produce much more cytosolic space and subsequent metabolism than resting B cells. GL7 staining of LPS-stimulated B cells showed heterogeneity in the degree of staining. Thus, cells used to prepare RNA for this real-time PCR experiment were a mixture of $GL7^{high}$ and $GL7^{low}$ cells. When these finding are taken into consideration, the reduction of *Cmah* expression in $GL7^{high}$ germinal center B cells could be more drastic. The expression of *Cd22*, an α2,6-linked Neu5Gc binding protein, on B cells was reduced to around 40% after 48 h, even though its cell surface expression was still comparable to that of unstimulated cells in flow cytometry (Fig. 4A and B).

Targeted disruption of the Cmah gene in mice. To further examine the in vivo function of Neu5Gc-bearing glycans, we targeted the *Cmah* gene in mice by inserting the neomycin resistance gene cassette into the second coding exon (Fig. 5A and B). Biochemical analysis of mouse tissues made it clear that gene inactivation was achieved, as homozygous null mice lacked enzyme expression in the liver ultracentrifugation supernatant, as shown by immunoblotting using antiserum against the N terminus of Cmah (Fig. 5C). We also did not detect a signal with a different molecular mass from the *Cmah*-disrupted allele. We further analyzed the effect of the enzyme deficiency on the level of its product by HPLC. *Cmah*-null tissues lacked detectable production of Neu5Gc throughout the normal adult mouse body (Fig. 5D). We concluded that the *Cmah* gene is indispensable for most of the cellular biosynthesis of Neu5Gc, as previously suggested in humans (6, 22). The development of the null mice appeared to be grossly normal; however, the numbers of null and heterozygote mutant offspring derived from F_1 crosses were subtly reduced from wild-type littermates in the rate expected from Mendelian rules (wild-type:heterozygote:null, 508:881:449), even though the mice were bred in a specific-pathogen-free mouse facility.

Normal B-cell maturation in *Cmah*-deficient mice. We found that Neu5Gc expression was severely repressed during B-cell activation in germinal centers, and thus we examined the development of the immune system in *Cmah*-null mice. In null mice, the values from blood counts and blood chemistry analyses were normal in every category examined (white blood cell, red blood cell, blood hemoglobin, hematocrit, mean corpuscular volume, mean corpuscular hemoglobin, mean corpuscular

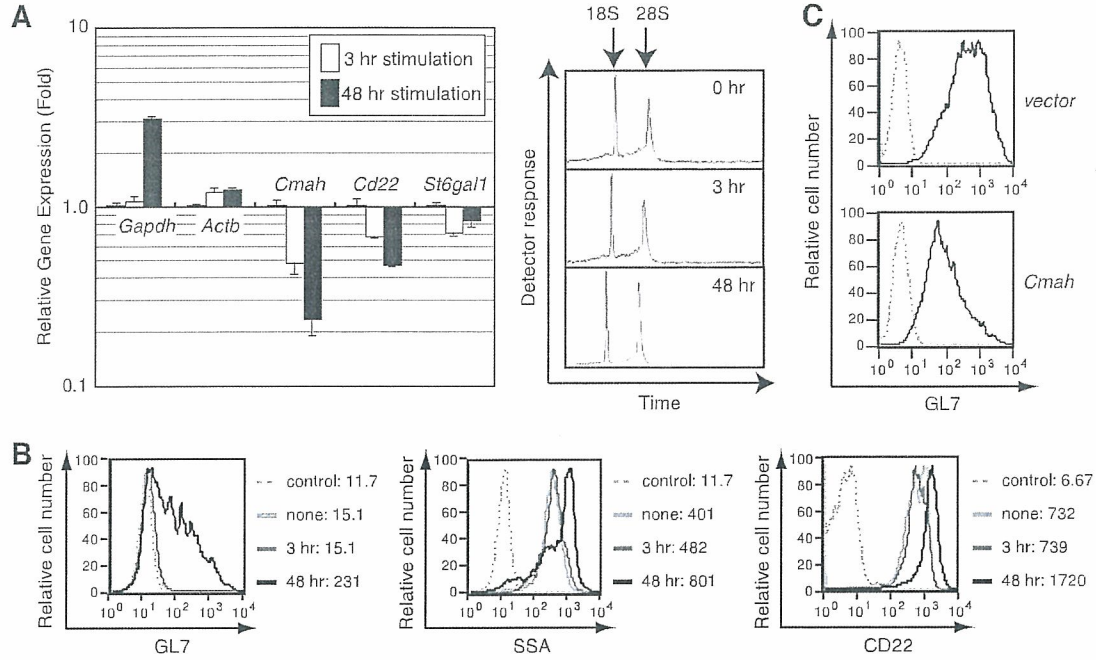

FIG. 4. Downregulation of *Cmah* mRNA in primary cultured B cell blasts, causing GL7 epitope expression. (A and B) Cmah repression caused by in vitro B-cell activation. Splenic B cells were stimulated with 30 μg/ml LPS for the indicated times. Reverse-transcribed cDNAs prepared from total RNA of these cells were subjected to real-time PCR analysis. The right box shows capillary electrophoresis analysis results indicating the lack of RNA degradation in the RNA used for cDNA synthesis. The expression levels of the mRNA of *Gapdh*, *Actb* (beta actin), *Cmah*, *Cd22*, and *St6gal1* are shown as the relative change compared with the mRNA expression in untreated B cells (A). The same set of cells that was used to prepare total RNA was stained with FITC-conjugated GL7, SSA, and anti-CD22 (B). The MFI of each stain is indicated at the right of each panel. (C) Reduced expression of the GL7 epitope by ectopic *Cmah* expression. *Cmah* was ectopically expressed in LPS-stimulated splenic B blasts using retrovirus. Retrovirus-infected cells were sorted and stained with FITC-conjugated GL7.

hemoglobin concentrate, and platelet). The development of immune cells in *Cmah*-null mice appeared to be grossly normal for T-cell and B-cell maturation, as indicated by routine flow cytometric analysis profiles. The indicators analyzed included the ratio of B1 to B2 cells, the ratio of marginal zone to follicular B cells, and the expression level of surface IgM, major histocompatibility complex class II (MHC-II), and CD22 (Fig. 5E; also see Table S2 in the supplemental material). We also examined the staining profile of activation markers for B cells. The only probe with a significant change in the null B cells was GL7 (Fig. 5F), which recognizes α2,6-linked Neu5Ac on LacNAc (Fig. 2C). Serum Ig measurements using the sandwich ELISA method revealed a significant ($P = 0.074$) increase in the serum IgG1 level of the *Cmah*-null population (Table 2).

Hyperreactive B cells in *Cmah*-deficient mice. We examined the mouse phenotype after immunization. When mice were immunized with the T-dependent antigen DNP-KLH or the T-independent (II) antigen DNP-Ficoll, the response to the T-independent antigen (serum titer against the hapten, DNP conjugated to BSA, by ELISA) was enhanced in null mice compared with controls, most prominently for IgM but also significantly for IgG3 (Fig. 6A). In contrast, the T-dependent response of the null group to DNP-KLH with potent complete Freund's adjuvant was not significantly different from that of the control group (Fig. 6B). Thus, the Neu5Gc deficiency in B cells resulted in a hyperresponsive phenotype to the T-independent antigen, indicating the importance of Neu5Gc-mediated negative regulation of B-cell activation. To further study the regulatory mechanism of the B-cell response by Neu5Gc-bearing glycans, mature splenic B cells were isolated and used in an in vitro proliferation assay with various stimuli. In this assay, compared with the cells from littermate controls, *Cmah*-null B cells proliferated robustly in response to the $F(ab')_2$ fragment against BCR (anti-μ chain), regardless of interleukin-4 (IL-4) addition (Fig. 6C). The FBS routinely used to support the cell culture contains around 5% Neu5Gc and represents a possible supply for *Cmah*-null cells. Therefore, we also examined the difference in proliferation using serum from chickens and humans, which contain only Neu5Ac as a Sia source (as determined by HPLC analysis [data not shown]). Under such conditions, *Cmah*-null B cells also showed augmented proliferation compared with control cells, although the degree of overall proliferation was much stronger in medium with FBS, perhaps because of differences in the growth factor(s) contained in each type of serum (data not shown). When anti-CD40 was used as the stimulus in a model mimicking T-dependent stimulation, B cells with both genotypes proliferated equally (data not shown); thus, Neu5Gc glycan-mediated regulation appeared to be stimulation dependent, and the effect seemed to be more related to T-independent activation. When T-cell proliferation was assessed using anti-CD3 as the stimulant, both *Cmah*-null and control splenic T cells proliferated to the same extent (see Fig. S2A in the supplemental material). No obvious bias toward either Th1 or Th2 was found in the cytokine production pattern of anti-CD3-stimulated *Cmah*-null T cells; however, a significant reduction of gamma

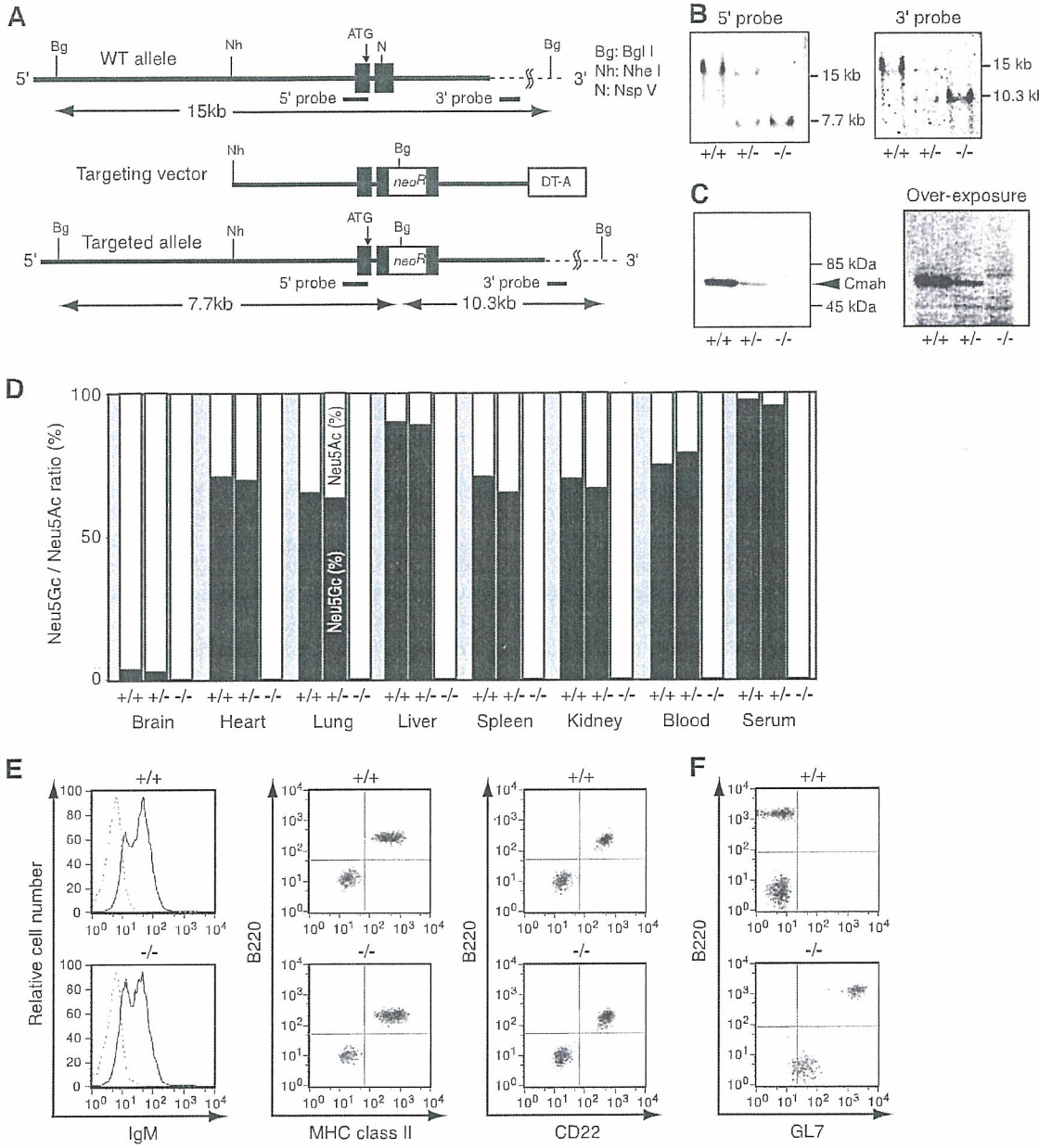

FIG. 5. Generation and biochemical analyses of *Cmah* knockout mice. (A) Allele for targeted *Cmah*. A targeting vector was created by inserting the *PGK-neoR* cassette into the NspV site of the second coding exon (exon 5) of the *Cmah* gene. (B) Genotype of homologous recombination of selected ES cell lines. The genotypes of G418-selected cell lines were determined by Southern blotting analysis of genomic DNA digested with BglI, using both radiolabeled 5′ internal and 3′ external probes. The genetic status of the *Cmah* allele is indicated as follows: +/+, wild type; +/−, heterozygote; and −/−, null (B to F). (C) Loss of Cmah enzyme demonstrated by immunoblotting analysis of liver cytosolic fractions. Ultracentrifugation supernatant fractions of livers were assessed for the expression of Cmah using anti-mouse Cmah immunoblotting. Staining of a ~67-kDa band (arrowhead) in wild-type and heterozygote livers represents the signal of Cmah, which is not detectable in *Cmah*-null liver samples. (D) Loss of Neu5Gc production throughout the body in mutated mice. Acid-hydrolyzed Sia from the indicated tissues was derivatized using DMB, and the ratios of Neu5Ac and Neu5Gc to total Sia were measured by reverse-phase HPLC. Solid columns represent the percentage of Neu5Gc in various tissues, and open columns represent the percentage of Neu5Ac. The detection limit for Neu5Gc in this assay was around 0.1%. (E) Flow cytometry profile of *Cmah*-null mice splenocytes. The expression of IgM, MHC-II (I-A and I-E), and CD22 on splenocytes from wild-type and *Cmah*-null mice was detected by flow cytometry. In anti-MHC-II and anti-CD22 staining, splenocytes were costained with anti-B220, a marker for B cells. (F) Strong expression of the GL7 epitope on *Cmah*-null mice B cells. Splenocytes from wild-type and *Cmah*-null mice were costained with anti-B220 and GL7 and subjected to flow cytometry.

interferon and IL-4 secretion was found in these cells (see Fig. S2B in the supplemental material). Based on these findings, we conclude that B cells from *Cmah*-deficient mice acquire hyperresponsiveness to stimuli, and thus the null animals show hyperresponsiveness (hyperproduction of antibodies) to the T-independent antigen.

Retrovirus-mediated rescue of hyperproliferative B-cell response in null mice. The LPS stimulation-dependent prolifer-

TABLE 2. Serum Ig isotype levels of nonimmunized *Cmah*-null mice

Isotype	Serum Ig level (μg/ml)[a]		
	Wild type	Heterozygote	*Cmah* null
IgM	169.6 ± 24.7	205.3 ± 38.9	190.0 ± 33.3
IgG1[b]	115.5 ± 14.9	151.3 ± 19.5	197.4 ± 41.2
IgG3	20.4 ± 2.3	23.9 ± 3.1	19.6 ± 3.8
IgA	242.7 ± 9.7	280.0 ± 29.2	260.2 ± 10.6

[a] Serum Ig levels were measured in nonimmunized mice at 7 to 13 weeks of age (at least 20 per genotype). Values are expressed as the means ± standard errors of the means.

[b] The serum IgG1 level was slightly increased in *Cmah*-null mice (Student's *t* test; $P = 0.074$ for wild type versus *Cmah* null).

ative response is also related to the T-independent response. In *Cmah*-null B cells, LPS stimulation caused enhanced proliferation (Fig. 7A). Given that LPS induces a considerable percentage of cells to progress through the cell cycle, retroviral infection-mediated gene rescue is possible. To determine whether the B-cell hyperreactivity was caused by the *Cmah* mutation, we expressed Cmah ectopically in LPS-stimulated proliferating *Cmah*-null B cells and found that the introduction of *Cmah* did result in repression of the hyperproliferation of *Cmah*-null B cells (Fig. 7B). This rescued hyperproliferative phenotype produced by ectopic Cmah expression in *Cmah*-null B cells indicates that the phenotypes in *Cmah*-null mice are caused by the loss of Cmah expression and probably not by effects on the expression of other genes owing to the insertion of the neomycin-resistance cassette during ES cell-based mutagenesis. This conclusion is also supported by the consistent phenotype resulting from the *Cmah*-disrupted allele in an extensively backcrossed C57BL/6J background. Moreover, our RT-PCR results confirmed equal expression levels of *Lrrc16* and *6330500D04Rik*, the genes located adjacent to the *Cmah* gene in the genome, in splenocytes of wild-type and *Cmah*-null mice (data not shown). To infect control and *Cmah*-encoding retrovirus, we used the same *Cmah*-null B-cell fractions. Since attenuated proliferation was found in *Cmah*-infected B-cell blasts, the augmented proliferation found in the *Cmah*-null B cells compared to the wild type (Fig. 6C) was not due to any subtle population difference in the B-cell fraction. Thus, we conclude that Cmah expression determines the proliferation of B cells when activated and that the difference in the in vivo response to the T-independent antigen is caused by differential expression of Neu5Gc in B cells.

Normal germinal center formation in the Cmah-deficient spleen. As shown in Fig. 5F, *Cmah*-null B cells strongly express the GL7 epitope, and GL7 has been used to detect the germinal center reaction in mice (5, 17, 41, 55). GL7-negative mature B cells turn GL7 positive during germinal center reactions upon T-dependent immunization. Germinal center B cells further develop to CD79b-positive memory B cells, which are no longer stained by GL7 (52). Therefore, it was of interest to assess whether these *Cmah*-null mice could undergo normal germinal center formation. PNA binds to glycan moieties with a terminal β-galactose residue at the core-1 branch of O-linked glycans, and it has been used as a marker for germinal center B cells (8). We compared the staining profiles of the two germinal center probes using spleen sections of wild-type and *Cmah*-null mice, either with or without SRBC immunization. In the wild-type spleen without immunization, PNA showed some staining in the marginal zone area, whereas GL7 did not (Fig. 8A). As expected from flow cytometric staining, GL7 widely stained the B-cell zone of the *Cmah*-null spleen even without immunization (Fig. 8A). When wild-type mice were immunized with SRBC, in addition to the marginal zone staining, intense PNA-positive germinal center follicles were observed. When PNA and GL7 staining results were compared on merged images, PNA appeared to stain a larger number of cells in the germinal center than did GL7, which stained a limited number of cells in the area, most probably centrocytes (Fig. 8B). In SRBC-immunized *Cmah*-null spleen, the staining pattern of GL7 was not different from that of the nonimmunized spleen section. These results confirmed that the appearance of GL7 epitope via the conversion of Neu5Gc to Neu5Ac is an activation-dependent event in the wild-type spleen, whereas *Cmah*-null mice lose Neu5Gc throughout; thus, *Cmah*-null spleen was stained by GL7 regardless of the immunization. In contrast, with GL7 staining, the *Cmah*-null spleen formed PNA-positive follicles that resembled the germinal centers of wild-type sections (Fig. 8B). These results suggest that *Cmah*-null mice could develop germinal centers upon SRBC immunization, which is consistent with the normal T-dependent antigen response found in *Cmah*-null mice.

Change in ligand expression for Siglecs in Cmah-null mice. The cell surface change in Sia species (Neu5Gc to Neu5Ac) by *Cmah* disruption could potentially cause a global change in sialylated glycan recognition throughout the body, as Neu5Gc is the predominant form of Sia in the mouse body, except in the neural system (Fig. 5D). In the immune system, various members of the Siglec family of Sia-binding lectins are expressed in a variety of immune cells. The counter-receptors for sialylated glycans affected by the C-5 position oxygen atom include sialoadhesin (Siglec-1, or CD169), which requires α2,3-linked Neu5Ac on galactose as a ligand (10), and CD22 (Siglec-2), which has a strong preference for Neu5Gc over Neu5Ac in the α2,6 linkage to LacNAc in mice (3, 26, 44, 50). To explore the change in ligand expression for Siglecs in *Cmah*-null mice, we prepared Siglec-Fc fusion probes that were free from intramolecular sialylation. In null B cells, the expression of the CD22 ligand was reduced roughly 20-fold compared with that in wild-type cells (Fig. 9A). We also histochemically examined the expression of the CD22 ligand on spleen sections from *Cmah*-null mice. Regardless of immunization, the mCD22-Fc probe failed to detect any staining in the sections of *Cmah*-null spleen, as in the germinal centers of immunized wild-type mice (Fig. 9B). Therefore, *Cmah* disruption caused the reduction of the optimal ligand for CD22. At the same time, ligand expression for sialoadhesin was greatly increased in *Cmah*-null mice (Fig. 9A). Sialoadhesin is expressed on macrophages, whereas CD22 is expressed on B cells. Ligand(s) for Siglec-G, another Siglec molecule presumably expressed on B cells, was not detected on B cells (data not shown); thus, the Siglec-related effects in *Cmah*-null B cells could be a loss of CD22 ligand.

Normal tyrosine phosphorylation upon BCR cross-linking in Cmah-null B cells. In addition to its biochemical activity as a lectin, CD22 also contains immunoreceptor tyrosine-based inhibitory motifs (ITIMs) in its cytoplasmic tail (4, 48). These ITIMs are phosphorylated as part of the phosphorylation

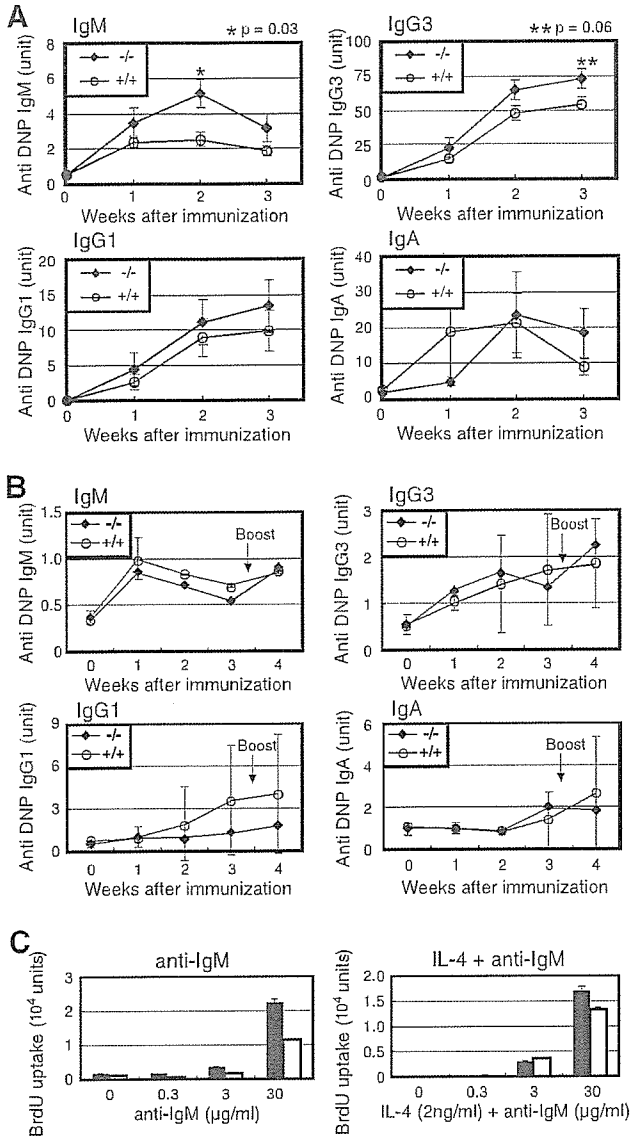

FIG. 6. Hyperresponsive phenotypes of *Cmah*-null mice. (A) T-independent hyperresponse of *Cmah*-null mice. DNP-Ficoll was used to immunize 8-week-old mice. Serum was collected each week and analyzed for reactivity with DNP-conjugated BSA coated on ELISA plates. The titer of hapten-reacting mouse Igs from each animal was determined by isotype-specific ELISA. The measured optical density at 405 nm was normalized to anti-DNP units by comparison with the value from standard pooled serum against DNP on the same plate. The results are presented as the mean responses of 10 animals for each genotype measured in two sets of experiments. The bars represent standard errors of the means. Open circles indicate the responses of wild-type mice, and filled diamonds indicate the responses of *Cmah*-null mice for each isotype. Genotypes are indicated as follows: +/+, wild-type; −/−, *Cmah*-null (A and B). (B) Normal T-dependent immune response of *Cmah*-null mice. DNP-KLH in complete Freund's adjuvant was used to immunize 8-week-old mice. The titers of hapten-reacting mouse Igs from each animal were determined by isotype-specific ELISA as above. Arrows indicate the time of secondary immunization with DNP-KLH. Open circles indicate the responses of wild-type mice, and filled diamonds indicate the responses of *Cmah*-null mice for each isotype. (C) In vitro hyperproliferation response of *Cmah*-null B cells. Splenic B cells from wild-type (open columns) and *Cmah*-null (filled columns) mice were assessed for proliferation using the $F(ab')_2$ fragment of anti-mouse IgM (μ chain) or anti-IgM plus 2 ng/ml IL-4 as stimulating reagents. After stimulation for 24 h, BrdU was added. Following incubation overnight, incorporated BrdU was detected by ELISA. Data are shown as the means of triplicate cultures, and the bars represent standard errors of the means. The results shown here were obtained in one of the experiments using 10% FBS-containing medium.

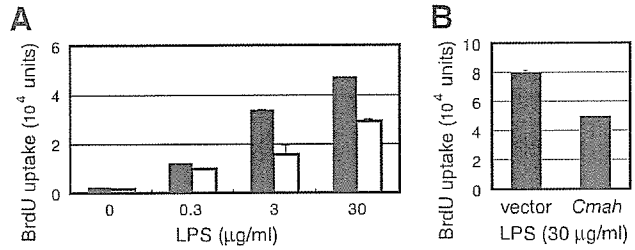

FIG. 7. Rescue of augmented proliferation of *Cmah*-null B cells by Cmah expression. (A) In vitro hyperproliferation response of *Cmah*-null B cells to LPS. Splenic B cells from wild-type (open columns) and *Cmah*-null mice (filled columns) were assessed for proliferation using LPS from *S. enterica* serovar Enteritidis as the stimulating reagent. Proliferation assays were performed as described in the legend of Fig. 6C. Data are shown as the means of triplicate cultures, and the bars represent standard errors of the means. (B) Reduction of B-cell proliferation by retrovirus-mediated Cmah expression. Cmah was ectopically expressed by mouse stem cell virus in *Cmah*-null splenic LPS B blasts. After being cultured for 2.5 days in the presence of 30 μg/ml LPS, the virus-infected B cells were subjected to a proliferation assay. As a control, cells were infected with an empty vector. Data are shown as the means of triplicate cultures, and the bars represent standard errors of the means.

cascade after BCR cross-linking. CD22 recruits SHP-1 tyrosine phosphatase to negatively regulate BCR signaling (11, 39). Given that CD22 is believed to be a regulator of BCR signaling and B-cell apoptosis (7, 13, 34, 58, 63) and that the level of BCR in *Cmah*-null mice was not different from that of the wild-type control (Fig. 5E), we analyzed the immediate-early CD22 phosphorylation status of mature B cells upon activation by BCR ligation. The overall tyrosine phosphorylation profile of B cells was not different for the two types of mice when the $F(ab')_2$ fragment of the anti-IgM (anti-μ chain) was used as a stimulant (Fig. 9C), although this may not be an optimal stimulant for CD22 phosphorylation (21). We further confirmed the tyrosine phosphorylation of CD22, possibly by Lyn kinase at the ITIM motif, upon BCR ligation. Consistently, the phosphorylation profile of CD22 assessed after immunoprecipitation by immunoblotting with an anti-phosphotyrosine antibody was almost identical in *Cmah*-null B cells and controls (Fig. 9D). In contrast, *Cmah*-null B cells showed augmented proliferation when a combination of tetradecanoyl phorbol acetate and ionomycin was used as a stimulant to directly activate classical protein kinase C(s). Thus, a downstream event of protein kinase C activation probably affects the hyperproliferative phenotype of *Cmah*-null B cells (Fig. 9E).

DISCUSSION

Change in Sia species in the germinal center. In the present study, we showed that activated B cells undergo a dramatic

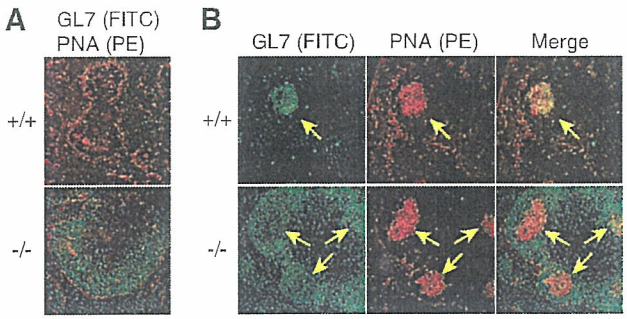

FIG. 8. Changes in staining of germinal center markers in normal or SRBC-immunized *Cmah*-null mice. (A) Histochemical analyses of spleen sections without immunization. Spleen sections from wild-type and *Cmah*-null mice were costained with FITC-conjugated GL7 and biotin-conjugated PNA visualized by R-PE-conjugated streptavidin. (B) Histochemical analyses of spleen sections after T-dependent immunization. Wild-type and *Cmah*-null mice were immunized with SRBC, and the spleens were removed 8 days after immunization. The frozen spleen sections were costained with FITC-conjugated GL7 and biotin-conjugated PNA followed by R-PE-conjugated streptavidin. Arrows indicate germinal centers. Genotypes are indicated as follows: +/+, wild type; −/−, *Cmah* null.

alteration of surface-sialylated glycans and that this alteration of Sia species from Neu5Gc to Neu5Ac can be probed with GL7. This is the first report regarding the epitope identification of GL7, which is routinely used to stain germinal center B cells in mice. We demonstrated that the GL7 epitope is the Neu5Acα2-6LacNAc-containing N-glycan, which is prominently expressed in activated B cells upon the repression of Cmah. Gain of GL7 epitope expression coincided with the loss of optimal ligand expression of CD22 in germinal center B cells, presumably centrocytes. Considering the rather strong degree of GL7 positivity in germinal center B cells in comparison with in vitro stimulated B-cell blasts, the degree of Cmah reduction might have been severe in these cells. In general, it is thought that Neu5Gc is easy to accumulate but difficult to turn over in cells. This is attributable to the one-way direction of the metabolic pathway; Neu5Gc is biosynthesized by Cmah from Neu5Ac (24, 36, 54), whereas no conversion activity was found to biosynthesize Neu5Ac from Neu5Gc. Therefore, the reduction of Neu5Gc found in the GL7-enriched germinal center cells is remarkable. Such rapid clearance of Neu5Gc could be attributable to several characteristics of germinal center cells. Most importantly, as shown in Fig. 3D, these cells repressed Cmah, the enzyme responsible for the de novo biosynthesis of Neu5Gc. Moreover, because lymphocytes are small cells with limited cytosolic space, the cytosolic pool of Sia in these cells is likely limited and easily turned over. In addition, centrocytes undergo extremely fast cell cycles (66), which probably leads to rapid passive dilution of the cytosolic pool in these cells. At the same time, new protein synthesis should be a primary event that happens in germinal center B cells, as shown by cDNA microarray analysis (51). The transcriptional repression of Cmah, together with these features of germinal center cells, could contribute to the efficient conversion of the major Sia species from Neu5Gc to Neu5Ac.

Negative regulation of B-cell activation by Cmah and its product, Neu5Gc. To clarify the biological role of Neu5Gc in vivo, we disrupted the *Cmah* gene in mice and examined their B-cell activation phenotypes. *Cmah*-null mice showed a hyperreactive B-cell phenotype to T-independent stimulation. In contrast, the T-dependent immunization response was similar to that in wild-type mice. This is consistent with the findings that Cmah expression is severely repressed in the germinal centers of wild-type spleen upon T-dependent immunization and that *Cmah*-null mice could develop follicles stained with PNA, another marker for germinal centers. Forced expression of Cmah caused repression of the proliferative response of *Cmah*-null B cells, indicating that Neu5Gc-containing sialoglycan functions to suppress B-cell reactivity though the mechanism is still unknown. This suppression via Neu5Gc-containing sialoglycan appears to be canceled by Cmah repression in germinal center B cells that are "activation committed" or "activation competent." The hyperreactive B-cell phenotypes observed in *Cmah*-null B cells could mirror differences in cellular reactivity between germinal center and nongerminal center B cells, as indicated by differential cell surface expression of the GL7 epitope (5).

Possible change in sialoglycan-receptor interaction in *Cmah*-null mice. As *Cmah* disruption results in a single oxygen atom change in these mice, it is expected that this mutation leaves both the Sia amount and Sia linkage intact in terms of sialoglycans, which could change the stability or turnover of the proteins modified with Sia (14). Although only limited information is available, sialyltransferases that biosynthesize sialylated glycans in the Golgi apparatus do not show strong preferences for CMP-Neu5Ac or CMP-Neu5Gc as substrates (59). When we probed linkage-specific protein sialylation by using α2,6-linked Sia-binding plant lectins such as *Sambucus nigra* agglutinin, we did not observe a change (data not shown). Thus, the molecular event affected in *Cmah*-null mice is likely to be lectin recognition of a single oxygen atom on sialoglycans expressed on the cell surface, although a single responsible lectin may not explain the phenotype. One of the candidate lectins as the receptor of sialoglycans is the Siglec family (9, 12, 62), though a yet-to-be-characterized Sia-binding molecule could be affected.

When ligand expression for Siglecs was detected using Siglec-Fc probes, *Cmah*-null mice lost optimal ligand expression for CD22 (Siglec-2). The ligand function of CD22 in a mouse model has been addressed in two different ways. One study was done using *St6gal1*-knockout mice (20), and another study analyzed gene-targeted mice expressing mutant CD22 molecules that do not interact with ligands (43). The phenotypes found in *Cmah*-null mice are considerably different from these two previous studies; therefore, *Cmah*-null phenotypes might be caused by the combination of loss/gain of a Sia-mediated interaction. Additional studies using a combination of various knockout strains related to sialoglycan recognition are required to address such possibilities.

Apart from the phenotypic contribution of CD22 to the assays in the present study, CD22 ligand expression is not static but is, instead, a regulated event during in vivo B-cell activation. We showed that mCD22-Fc probe staining was downregulated in germinal centers. Moreover, it was reported that in vitro activated human B cells unmask CD22 from a *cis*-ligand (45). Thus, the regulation of CD22 ligand expression

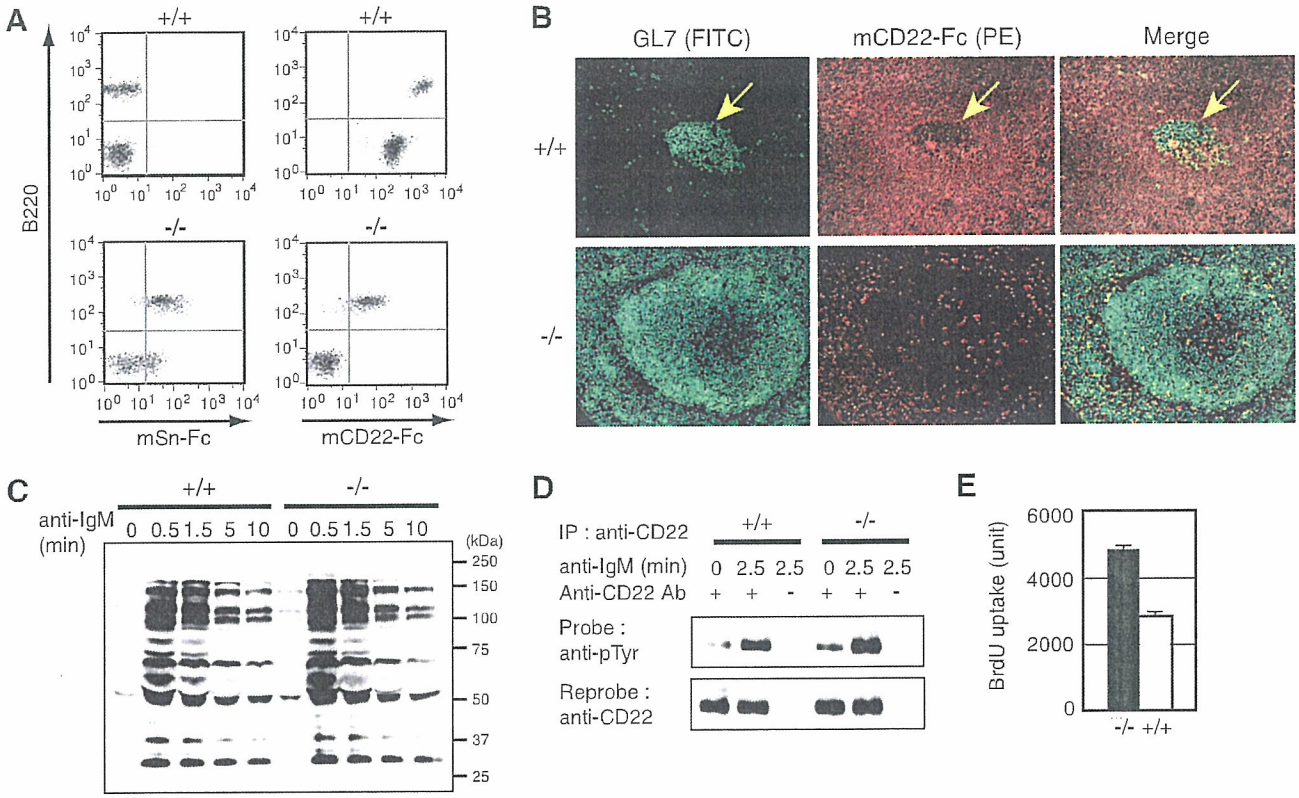

FIG. 9. Loss of optimal CD22 ligand and normal immediate response upon BCR cross-linking in *Cmah*-null mice. (A) Loss of optimal ligand for CD22 in *Cmah*-null mice. The expression of surface ligands for sialoadhesin and CD22 was detected by flow cytometry. Splenocytes from wild-type and *Cmah*-null mice were costained with FITC-conjugated anti-B220 and mSn/mCD22-Fc precomplexed with R-PE-conjugated anti-human IgG. Wild-type B cells were strongly stained with mCD22-Fc. In contrast, the level of mCD22-Fc staining showed a marked decrease in *Cmah*-null mice. The weak signal found on *Cmah*-null splenocytes was detected only with the chimeric probe mCD22-Fc prepared from Lec2 cell culture medium and not with the probe prepared from COS7 cells, possibly because of the autosialylation. (B) Histochemical analyses of CD22 ligand expression in spleen sections. Spleen sections from wild-type and *Cmah*-null mice 8 days after SRBC immunization were costained with FITC-conjugated GL7 and mCD22-Fc precomplexed with R-PE-conjugated anti-human IgG. Arrows indicate germinal centers. (C) Overall tyrosine phosphorylation upon anti-IgM stimulation. Splenic B cells from wild-type and *Cmah*-null mice were stimulated with the $F(ab')_2$ fragment of anti-mouse IgM (μ chain) for the indicated times. Whole-cell lysates were subjected to immunoblotting with antiphosphotyrosine antibody (PT-66). (D) Phosphorylation of CD22. Splenic B cells were stimulated with the $F(ab')_2$ fragment of anti-mouse IgM (μ chain) for the indicated times. The cell lysates were subjected to immunoprecipitation with anti-CD22 antibody (Cy34.1). The precipitated proteins were immunoblotted with antiphosphotyrosine (pTyr) antibody (PT-66) and then reprobed with anti-CD22 polyclonal antibody. (E) In vitro hyperproliferation response of *Cmah*-null B cells to calcium signaling. Splenic B cells were assessed for proliferation using tetradecanoyl phorbol acetate (10 ng/ml) plus ionomycin (5 μg/ml) as stimulating reagents. The proliferation assay was performed as described in the legend of Fig. 6C. The open column represents the mean proliferation of wild-type B cells, and the filled column represents the mean proliferation of *Cmah*-null B cells. The bars represent the standard errors of the mean for triplicate cultures. +/+, wild type; −/−, *Cmah* null; IP, immunoprecipitation.

could be an important event to modulate B-cell activation in vivo.

Loss of Neu5Gc in relation to human deficiency for the *CMAH* gene. *Homo sapiens* is the sole mammalian species that lacks Neu5Gc expression throughout the body; indeed, Neu5Gc is antigenic to humans (31). This is a striking difference between humans and chimpanzees, which express Neu5Gc as the major species of Sia throughout their bodies. Recently, it was shown that, unlike gene expression in the extant great apes, the *CMAH* gene is inactivated in humans (6, 22). Here, we demonstrated that Cmah is the sole enzyme responsible for the production of Neu5Gc in cells since our mouse model reproduced the human-like deficiency in Neu5Gc biosynthesis. This result confirmed that a genetic mutation in the human lineage caused the lack of Neu5Gc in humans.

Sia is commonly used in the host recognition system of microbes, and human-specific microbes are reported to recognize epitope(s) containing Neu5Ac on human cells. The mouse described here is thus the first mammalian line that could be used as an animal model system to assess Sia-targeted human infectious diseases (15).

ACKNOWLEDGMENTS

We thank Motomi Osato and Yoshiaki Itoh for the blood chemistry and blood counting experiments. We also thank Ajit Varki, Takeshi Tsubata, and Reiji Kannagi for helpful discussions during the preparation of the manuscript.

This work was supported by CREST, Japanese Science and Technology; a grant-in-aid program from the Ministry of Education, Culture, Sports, Science, and Technology of Japan; and RIKEN.

REFERENCES

1. **Alizadeh, A. A., M. B. Eisen, R. E. Davis, C. Ma, I. S. Lossos, A. Rosenwald, J. C. Boldrick, H. Sabet, T. Tran, X. Yu, J. I. Powell, L. Yang, G. E. Marti, T. Moore, J. Hudson, Jr., L. Lu, D. B. Lewis, R. Tibshirani, G. Sherlock, W. C. Chan, T. C. Greiner, D. D. Weisenburger, J. O. Armitage, R. Warnke, R. Levy, W. Wilson, M. R. Grever, J. C. Byrd, D. Botstein, P. O. Brown, and L. M. Staudt.** 2000. Distinct types of diffuse large B-cell lymphoma identified by gene expression profiling. Nature **403**:503–511.
2. **Baum, L. G., K. Derbin, N. L. Perillo, T. Wu, M. Pang, and C. Uittenbogaart.** 1996. Characterization of terminal sialic acid linkages on human thymocytes. Correlation between lectin-binding phenotype and sialyltransferase expression. J. Biol. Chem. **271**:10793–10799.
3. **Blixt, O., B. E. Collins, I. M. Van Den Nieuwenhof, P. R. Crocker, and J. C. Paulson.** 2003. Sialoside specificity of the Siglec family assessed using novel multivalent probes: identification of potent inhibitors of myelin associated glycoproteins. J. Biol. Chem. **278**:31007–31019.
4. **Bubl, A. M., and J. C. Cambier.** 1997. Co-receptor and accessory regulation of B-cell antigen receptor signal transduction. Immunol. Rev. **160**:127–138.
5. **Cervenak, L., A. Magyar, R. Boja, and G. Laszlo.** 2001. Differential expression of GL7 activation antigen on bone marrow B cell subpopulations and peripheral B cells. Immunol. Lett. **78**:89–96.
6. **Chou, H. H., H. Takematsu, S. Diaz, J. Iber, E. Nickerson, K. L. Wright, E. A. Muchmore, D. L. Nelson, S. T. Warren, and A. Varki.** 1998. A mutation in human CMP-sialic acid hydroxylase occurred after the Homo-Pan divergence. Proc. Natl. Acad. Sci. USA **95**:11751–11756.
7. **Clark, E. A.** 1993. CD22, a B cell-specific receptor, mediates adhesion and signal transduction. J. Immunol. **150**:4715–4718.
8. **Coico, R. F., B. S. Bhogal, and G. J. Thorbecke.** 1983. Relationship of germinal centers in lymphoid tissue to immunologic memory. VI. Transfer of B cell memory with lymph node cells fractionated according to their receptors for peanut agglutinin. J. Immunol. **131**:2254–2257.
9. **Crocker, P. R.** 2002. Siglecs: sialic-acid-binding immunoglobulin-like lectins in cell-cell interactions and signalling. Curr. Opin. Struct. Biol. **12**:609–615.
10. **Crocker, P. R., S. Kelm, C. Dubois, B. Martin, A. S. McWilliam, D. M. Shotton, J. C. Paulson, and S. Gordon.** 1991. Purification and properties of sialoadhesin, a sialic acid-binding receptor of murine tissue macrophages. EMBO J. **10**:1661–1669.
11. **Crocker, P. R., and A. Varki.** 2001. Siglecs in the immune system. Immunology **103**:137–145.
12. **Crocker, P. R., and A. Varki.** 2001. Siglecs, sialic acids and innate immunity. Trends Immunol. **22**:337–342.
13. **Cyster, J. G., and C. C. Goodnow.** 1997. Tuning antigen receptor signaling by CD22: Integrating cues from antigens and the microenvironment. Immunity **6**:509–517.
14. **Ellies, L. G., D. Ditto, G. G. Levy, M. Wahrenbrock, D. Ginsburg, A. Varki, D. T. Le, and J. D. Marth.** 2002. Sialyltransferase ST3Gal-IV operates as a dominant modifier of hemostasis by concealing asialoglycoprotein receptor ligands. Proc. Natl. Acad. Sci. USA **99**:10042–10047.
15. **Gagneux, P., and A. Varki.** 1999. Evolutionary considerations in relating oligosaccharide diversity to biological function. Glycobiology **9**:747–755.
16. **Han, H., D. J. Bearss, L. W. Browne, R. Calaluce, R. B. Nagle, and D. D. Von Hoff.** 2002. Identification of differentially expressed genes in pancreatic cancer cells using cDNA microarray. Cancer Res. **62**:2890–2896.
17. **Han, S., S. R. Dillon, B. Zheng, M. Shimoda, M. S. Schlissel, and G. Kelsoe.** 1997. V(D)J recombinase activity in a subset of germinal center B lymphocytes. Science **278**:301–305.
18. **Han, S., B. Zheng, D. G. Schatz, E. Spanopoulou, and G. Kelsoe.** 1996. Neoteny in lymphocytes: Rag1 and Rag2 expression in germinal center B cells. Science **274**:2094–2097.
19. **Hathcock, K. S., C. E. Pucillo, G. Laszlo, L. Lai, and R. J. Hodes.** 1995. Analysis of thymic subpopulations expressing the activation antigen GL7: expression, genetics, and function. J. Immunol. **155**:4575–4581.
20. **Hennet, T., D. Chui, J. C. Paulson, and J. D. Marth.** 1998. Immune regulation by the ST6Gal sialyltransferase. Proc. Natl. Acad. Sci. USA **95**:4504–4509.
21. **Hokazono, Y., T. Adachi, M. Wabl, N. Tada, T. Amagasa, and T. Tsubata.** 2003. Inhibitory coreceptors activated by antigens but not by anti-Ig heavy chain antibodies install requirement of costimulation through CD40 for survival and proliferation of B cells. J. Immunol. **171**:1835–1843.
22. **Irie, A., S. Koyama, Y. Kozutsumi, T. Kawasaki, and A. Suzuki.** 1998. The molecular basis for the absence of *N*-glycolylneuraminic acid in humans. J. Biol. Chem. **273**:15866–15871.
23. **Itohara, S., P. Mombaerts, J. Lafaille, J. Iacomini, A. Nelson, A. R. Clarke, M. L. Hooper, A. Farr, and S. Tonegawa.** 1993. T cell receptor delta gene mutant mice: independent generation of alpha beta T cells and programmed rearrangements of gamma delta TCR genes. Cell **72**:337–348.
24. **Kawano, T., S. Koyama, H. Takematsu, Y. Kozutsumi, H. Kawasaki, S. Kawashima, T. Kawasaki, and A. Suzuki.** 1995. Molecular cloning of cytidine monophospho-*N*-acetylneuraminic acid hydroxylase. Regulation of species- and tissue-specific expression of *N*-glycolylneuraminic acid. J. Biol. Chem. **270**:16458–16463.
25. **Kawano, T., Y. Kozutsumi, T. Kawasaki, and A. Suzuki.** 1994. Biosynthesis of *N*-glycolylneuraminic acid-containing glycoconjugates. Purification and characterization of the key enzyme of the cytidine monophospho-*N*-acetylneuraminic acid hydroxylation system. J. Biol. Chem. **269**:9024–9029.
26. **Kelm, S., A. Pelz, R. Schauer, M. T. Filbin, S. Tang, M. E. de Bellard, R. L. Schnaar, J. A. Mahoney, A. Hartnell, P. Bradfield, et al.** 1994. Sialoadhesin, myelin-associated glycoprotein and CD22 define a new family of sialic acid-dependent adhesion molecules of the immunoglobulin superfamily. Curr. Biol **4**:965–972.
27. **Koyama, S., T. Yamaji, H. Takematsu, T. Kawano, Y. Kozutsumi, A. Suzuki, and T. Kawasaki.** 1996. A naturally occurring 46-amino-acid deletion of cytidine monophospho-*N*-acetylneuraminic acid hydroxylase leads to a change in the intracellular distribution of the protein. Glycoconj. J. **13**:353–358.
28. **Laszlo, G., K. S. Hathcock, H. B. Dickler, and R. J. Hodes.** 1993. Characterization of a novel cell-surface molecule expressed on subpopulations of activated T and B cells. J. Immunol. **150**:5252–5262.
29. **Lossos, I. S., A. A. Alizadeh, M. B. Eisen, W. C. Chan, P. O. Brown, D. Botstein, L. M. Staudt, and R. Levy.** 2000. Ongoing immunoglobulin somatic mutation in germinal center B cell-like but not in activated B cell-like diffuse large cell lymphomas. Proc. Natl. Acad. Sci. USA **97**:10209–10213.
30. **MacLennan, I. C.** 1994. Germinal centers. Annu. Rev. Immunol. **12**:117–139.
31. **Martin, M. J., A. Muotri, F. Gage, and A. Varki.** 2005. Human embryonic stem cells express an immunogenic nonhuman sialic acid. Nat. Med. **11**:228–232.
32. **McHeyzer-Williams, L. J., M. Cool, and M. G. McHeyzer-Williams.** 2000. Antigen-specific B cell memory: expression and replenishment of a novel $B220^-$ memory B cell compartment. J. Exp. Med. **191**:1149–1166.
33. **McHeyzer-Williams, L. J., D. J. Driver, and M. G. McHeyzer-Williams.** 2001. Germinal center reaction. Curr. Opin. Hematol. **8**:52–59.
34. **Mills, D. M., J. C. Stolpa, and J. C. Cambier.** 2004. Cognate B cell signaling via MHC class II: differential regulation of B cell antigen receptor and MHC class II/Ig-$\alpha\beta$ signaling by CD22. J. Immunol. **172**:195–201.
35. **Morita, S., T. Kojima, and T. Kitamura.** 2000. Plat-E: an efficient and stable system for transient packaging of retroviruses. Gene Ther. **7**:1063–1066.
36. **Muchmore, E. A., M. Milewski, A. Varki, and S. Diaz.** 1989. Biosynthesis of *N*-glycolylneuraminic acid. The primary site of hydroxylation of *N*-acetylneuraminic acid is the cytosolic sugar nucleotide pool. J. Biol. Chem. **264**:20216–20223.
37. **Muramatsu, M., V. S. Sankaranand, S. Anant, M. Sugai, K. Kinoshita, N. O. Davidson, and T. Honjo.** 1999. Specific expression of activation-induced cytidine deaminase (AID), a novel member of the RNA-editing deaminase family in germinal center B cells. J. Biol. Chem. **274**:18470–18476.
38. **Murasawa, M., S. Okada, S. Obata, M. Hatano, H. Moriya, and T. Tokuhisa.** 2002. GL7 defines the cycling stage of pre-B cells in murine bone marrow. Eur. J. Immunol. **32**:291–298.
39. **Nitschke, L.** 2005. The role of CD22 and other inhibitory co-receptors in B-cell activation. Curr. Opin. Immunol. **17**:290–297.
40. **Novoradovskaya, N., M. L. Whitfield, L. S. Basehore, A. Novoradovsky, R. Pesich, J. Usary, M. Karaca, W. K. Wong, O. Aprelikova, M. Fero, C. M. Perou, D. Botstein, and J. Braman.** 2004. Universal reference RNA as a standard for microarray experiments. BMC Genomics **5**:20.
41. **Pasare, C., and R. Medzhitov.** 2005. Control of B-cell responses by Toll-like receptors. Nature **438**:364–368.
42. **Paulson, J. C., J. Weinstein, and A. Schauer.** 1989. Tissue-specific expression of sialyltransferases. J. Biol. Chem. **264**:10931–10934.
43. **Poe, J. C., Y. Fujimoto, M. Hasegawa, K. M. Haas, A. S. Miller, I. G. Sanford, C. B. Bock, M. Fujimoto, and T. F. Tedder.** 2004. CD22 regulates B lymphocyte function in vivo through both ligand-dependent and ligand-independent mechanisms. Nat. Immunol. **5**:1078–1087.
44. **Powell, L. D., and A. Varki.** 1994. The oligosaccharide binding specificities of CD22 beta, a sialic acid-specific lectin of B cells. J. Biol. Chem. **269**:10628–10636.
45. **Razi, N., and A. Varki.** 1998. Masking and unmasking of the sialic acid-binding lectin activity of CD22 (Siglec-2) on B lymphocytes. Proc. Natl. Acad. Sci. USA **95**:7469–7474.
46. **Reichert, R. A., W. M. Gallatin, I. L. Weissman, and E. C. Butcher.** 1983. Germinal center B cells lack homing receptors necessary for normal lymphocyte recirculation. J. Exp. Med. **157**:813–827.
47. **Schauer, R.** 1982. Sialic acids: chemistry, metabolism and function. Cell biology monographs, vol. 10. Springer-Verlag, New York, NY.
48. **Schulte, R. J., M. A. Campbell, W. H. Fischer, and B. M. Sefton.** 1992. Tyrosine phosphorylation of CD22 during B cell activation. Science **258**:1001–1004.
49. **Schwarzkopf, M., K. P. Knobeloch, E. Rohde, S. Hinderlich, N. Wiechens, L. Lucka, I. Horak, W. Reutter, and R. Horstkorte.** 2002. Sialylation is essential for early development in mice. Proc. Natl. Acad. Sci. USA **99**:5267–5270.
50. **Sgroi, D., A. Varki, S. Braesch-Andersen, and I. Stamenkovic.** 1993. CD22,

a B cell-specific immunoglobulin superfamily member, is a sialic acid-binding lectin. J. Biol. Chem. **268**:7011–7018.
51. **Shaffer, A. L., A. Rosenwald, E. M. Hurt, J. M. Giltnane, L. T. Lam, O. K. Pickeral, and L. M. Staudt.** 2001. Signatures of the immune response. Immunity **15**:375–385.
52. **Shapiro-Shelef, M., K. I. Lin, L. J. McHeyzer-Williams, J. Liao, M. G. McHeyzer-Williams, and K. Calame.** 2003. Blimp-1 is required for the formation of immunoglobulin secreting plasma cells and pre-plasma memory B cells. Immunity **19**:607–620.
53. **Shaw, L., and R. Schauer.** 1988. The biosynthesis of *N*-glycolylneuraminic acid occurs by hydroxylation of the CMP-glycoside of *N*-acetylneuraminic acid. Biol. Chem. Hoppe-Seyler **369**:477–486.
54. **Shaw, L., and R. Schauer.** 1989. Detection of CMP-*N*-acetylneuraminic acid hydroxylase activity in fractionated mouse liver. Biochem. J. **263**: 355–363.
55. **Shih, T. A., E. Meffre, M. Roederer, and M. C. Nussenzweig.** 2002. Role of BCR affinity in T cell dependent antibody responses in vivo. Nat. Immunol. **3**:570–575.
56. **Sjoberg, E. R., L. D. Powell, A. Klein, and A. Varki.** 1994. Natural ligands of the B cell adhesion molecule CD22 beta can be masked by 9-O-acetylation of sialic acids. J. Cell Biol. **126**:549–562.
57. **Takematsu, H., S. Diaz, A. Stoddart, Y. Zhang, and A. Varki.** 1999. Lysosomal and cytosolic sialic acid 9-*O*-acetylesterase activities can be encoded by one gene via differential usage of a signal peptide-encoding exon at the N terminus. J. Biol. Chem. **274**:25623–25631.
58. **Tedder, T. F., J. Tuscano, S. Sato, and J. H. Kehrl.** 1997. CD22, a B lymphocyte-specific adhesion molecule that regulates antigen receptor signaling. Annu. Rev. Immunol. **15**:481–504.
59. **Tsuji, S.** 1996. Molecular cloning and functional analysis of sialyltransferases. J. Biochem. (Tokyo) **120**:1–13.
60. **Varki, A.** 1992. Diversity in the sialic acids Glycobiology **2**:25–40. (Erratum, **2**:168.)
61. **Varki, A.** 1997. Sialic acids as ligands in recognition phenomena. FASEB J. **11**:248–255.
62. **Varki, A., and T. Angata.** 2006 Siglecs—the major subfamily of I-type lectins. Glycobiology **16**:1R–27R.
63. **Wakabayashi, C., T. Adachi, J. Wienands, and T. Tsubata.** 2002. A distinct signaling pathway used by the IgG-containing B cell antigen receptor. Science **298**:2392–2395.
64. **Wuensch, S. A., R. Y. Huang, J. Ewing, X. Liang, and J. T. Lau.** 2000. Murine B cell differentiation is accompanied by programmed expression of multiple novel β-galactoside α2, 6-sialyltransferase mRNA forms. Glycobiology **10**: 67–75.
65. **Yamaji, T., T. Teranishi, M. S. Alphey, P. R. Crocker, and Y. Hashimoto.** 2002. A small region of the natural killer cell receptor, Siglec-7, is responsible for its preferred binding to α2,8-disialyl and branched α2,6-sialyl residues. A comparison with Siglec-9. J. Biol. Chem. **277**:6324–6332.
66. **Zhang, J., I. C. MacLennan, Y. J. Liu, and P. J. Lane.** 1988. Is rapid proliferation in B centroblasts linked to somatic mutation in memory B cell clones? Immunol. Lett. **18**:297–299.

Available online at www.sciencedirect.com
ScienceDirect
Toxicology Letters 167 (2006) 106–113
Toxicology Letters
www.elsevier.com/locate/toxlet

Altered gene expression of transcriptional regulatory factors in tumor marker-positive cells during chemically induced hepatocarcinogenesis

Shigehiro Osada[a,b,*,1], Ayako Naganawa[a,1], Masashi Misonou[a], Soken Tsuchiya[c,d], Shigero Tamba[c], Yasushi Okuno[d,e], Jun-ichi Nishikawa[a], Kimihiko Satoh[f], Masayoshi Imagawa[b], Gozoh Tsujimoto[e], Yukihiko Sugimoto[c], Tsutomu Nishihara[a]

[a] *Laboratory of Environmental Biochemistry, Graduate School of Pharmaceutical Sciences, Osaka University, 1-6 Yamada-Oka, Suita, Osaka 565-0871, Japan*
[b] *Department of Molecular Biology, Graduate School of Pharmaceutical Sciences, Nagoya City University, 3-1 Tanabe-dori, Mizuho-ku, Nagoya, Aichi 467-8603, Japan*
[c] *Department of Physiological Chemistry, Graduate School of Pharmaceutical Sciences, Kyoto University, 46-29 Yoshida Shimoadachi-cho, Sakyo-ku, Kyoto 606-8501, Japan*
[d] *Department of Pharmacoinformatics, Graduate School of Pharmaceutical Sciences, Kyoto University, 46-29 Yoshida Shimoadachi-cho, Sakyo-ku, Kyoto 606-8501, Japan*
[e] *Department of Genomic Drug Discovery Science, Graduate School of Pharmaceutical Sciences, Kyoto University, 46-29 Yoshida Shimoadachi-cho, Sakyo-ku, Kyoto 606-8501, Japan*
[f] *Department of Organic Function, Hirosaki University, School of Health Science, Hon-Cho 66-1, Hirosaki 036-8564, Japan*

Received 10 August 2006; received in revised form 29 August 2006; accepted 29 August 2006
Available online 25 September 2006

Abstract

Glutathione-*S*-transferase placental form (GST-P) is markedly and specifically inducible in rat chemical hepatocarcinogenesis and is a reliable marker protein for pre-neoplasia. To gain insights into the molecular mechanisms at the early stage of hepatocarcinogenesis and hepatotoxicity, we investigated the gene expression profile by DNA microarray analysis. We prepared RNA from GST-P-positive foci in three individual rats and compared with normal liver sections from three individual rats, and labeled RNA was individually hybridized onto Affymetrix GeneChip Rat Expression Array 230A. DNA microarray analysis showed distinctly different profiles of dysregulated gene expression and supported the previous finding that some enzymes involved in metabolism and detoxification are overexpressed and suppressed. Here we discovered that several DNA-binding transcription factors and cofactors, including sterol-regulatory-element binding protein 1 (SREBP1) and Wilms' tumour 1 (WT1)-interacting protein, and their target genes were dysregulated in GST-P-positive foci. Moreover, genes involved in chromatin components, histone modification enzymes, and centrosome duplication were highly expressed. These genes were not previously known to be up-regulated during chemically induced hepatocarcinogenesis. DNA microarray analysis using RNA prepared from tumor marker-positive foci and control tissues provided a candidate gene link to the early stage of carcinogenesis and hepatotoxicity.

Keywords: Chemical hepatocarcinogenesis; Tumor marker; Gene expression; Transcription factor; Chromatin; Histone

* Corresponding author at: Department of Molecular Biology, Graduate School of Pharmaceutical Sciences, Nagoya City University, 3-1 Tanabe-dori, Mizuho-ku, Nagoya, Aichi 467-8603, Japan. Tel.: +81 52 836 3456; fax: +81 52 836 3456.
E-mail address: osada@phar.nagoya-cu.ac.jp (S. Osada).
[1] These authors contributed equally to this work.

0378-4274/$ – see front matter © 2006 Elsevier Ireland Ltd. All rights reserved.
doi:10.1016/j.toxlet.2006.08.014

1. Introduction

Rat glutathione-*S*-transferase placental form (GST-P) is a phase II detoxification enzyme and its expression is completely repressed in normal liver. GST-P is also a well-known tumor marker that is specifically induced during chemical hepatocarcinogenesis in rats (Sato, 1989; Satoh et al., 1985). GST-P expressed single cells are detected in the liver after treatment of diethylnitrosamine (DEN) and might be precursors of preneoplastic foci and nodules (Satoh et al., 1989; Satoh et al., 2005). Hepatocyte nodules in six models of liver carcinogenesis were analyzed and the amount of GST-P was elevated in all types of nodules (Eriksson et al., 1983). Measurement of GST-P-positive foci is rapid detection of carcinogenic agents in the medium-term rat liver bioassay (Ito test), which is considered to be a reliable tool for prediction of promoting or reducing activity of chemicals on hepatocarcinogenesis. Over 300 chemicals have already observed and this test was recommended as an alternative to long-term carcinogenicity testing at the International Conference on Harmonization (ICH) (Ito et al., 2003). GST-P-positive foci are induced by not only DEN but many chemicals. Gamma-glutamyltranspeptidase is also expressed in GST-P-positive foci derived from precursor cells and GST-P-positive foci are important for detoxification for carcinogen (Satoh et al., 2005). Carcinogenic activity of nitroso compounds, including DEN, is well studied, but the mechanisms of hepatotoxicity of these compounds are poorly understood. Analysis of GST-P-positive foci is valuable for the understanding of the molecular mechanisms of hepatocarcinogenesis, detoxification and hepatotoxicity.

Transgenic rats using the regulatory element of the GST-P gene revealed that a gene involved in liver cell transformation is not physically linked with the GST-P gene, but the expression is regulated by common transcription factors (Morimura et al., 1993). Further, we identified the enhancer element responsible for tumor-specific expression of the GST-P gene (Sakai and Muramatsu, 2005; Suzuki et al., 1995). This indicates that analysis of the expression profile in GST-P-positive foci leads to the identification of the responsible gene for liver cancer and understanding the mechanism of hepatocarcinogenesis.

Carcinogenesis is a genetic and epigenetic disease arising from multiple molecular changes and these events lead to changes in gene expressions. Recently, it was reported that specific differences in the gene expression profile revealed by cDNA microarray analysis of GST-P-positive foci and the surrounding tissue, and metabolic enzymes were found as up- and down-regulated genes (Suzuki et al., 2004). Direct comparisons of gene expressions between normal liver and chemically induced preneoplastic foci provide more useful information related to the molecular mechanisms of carcinogenesis. Although genes involved in transcriptional regulation are one of the most important factors in carcinogenesis, their expression levels are generally lower than those of metabolic enzymes and are hard to evaluate by DNA microarray analysis.

In this study, we conducted microarray analysis of mRNA from GST-P-positive foci in three individual rats and compared with normal liver sections from three individual rats. Labeled RNA was individually hybridized onto GeneChip Rat Expression Array 230A, and several differentially expressed genes were found to be involved in transcriptional regulation, which were not previously known to be regulated during chemically induced hepatocarcinogenesis.

2. Materials and methods

2.1. Chemical hepatocarcinogenesis of rats

Carcinogenic experiments were done according to the Solt–Farber protocol (Solt and Farber, 1976). Experiments were initiated by intraperitoneal injection of DEN (200 mg/kg) (Wako Pure Chemical Industries, Ltd., Osaka, Japan) into 5-week-old Sprague–Dawley rats. After the animals had been fed basal diets for 2 weeks, they were changed to basal diets containing 0.02% 2-acetylaminofluorene (Nacalai Tesque, Kyoto, Japan). Three weeks after DEN injection, partial hepatectomy was performed and livers were extirpated 8 weeks after DEN injection. Control rats were injected with saline and fed basal diets. All animal care and handling procedures were approved by the animal care and use committee of Osaka University.

2.2. Preparation of RNA from rat liver

To map the exact location of GST-P-positive foci, one of the serial frozen sections (10 μm) from the liver was treated with rabbit anti-GST-P antibody and immunohistochemical staining was performed with the DAKO ENVISION System (DAKO Co., Tokyo, Japan). RNA was prepared from the area corresponding to GST-P-positive foci in hyperplastic nodules induced in three individual rats or sections from three control rats by RNeasy Mini Kit (QIAGEN, Hilden, Germany).

2.3. Oligonucleotide microarray and data analysis

Target RNA amplification and labeling with biotinylated nucleotides were carried out using MEGAscript T7 Kit (Ambion, Austin, TX) and Enzo BioArray High Yield RNA Transcript Labeling Kit (Enzo Diagnostics, Farmingdale, NY) as specified by the manufacturer. The quality and

size distribution of the targets were determined using the Agilent 2100 Bioanalyzer (Agilent Technologies, Palo Alto, CA). Labeled and fragmented RNA of individual rats was hybridized onto GeneChip Rat Expression Array 230A (Affymetrix, Santa Clara, CA) using standard methods. We calculated the background correction and normalization of the array data using Robust Multi-Array (RMA) method in the R package. Statistics of differential expression between genes was estimated using the linear modeling features of the limma library of the R. Limma computes p-values of moderated t-statistics by emprical Bayes shrinkage of the standard error toward a common value.

3. Results and discussion

3.1. Detection of GST-P-positive foci

To examine the expression profile of GST-P-positive foci during hepatocarcinogenesis, hyperplastic nodule-induced rats were prepared according to the Solt–Farber procedure (Solt and Farber, 1976). Eight weeks after DEN treatment, the livers, which had a large number of foci and nodules, were excised and immunohistochemical experiments indicated that an approximately 70–80% region contained GST-P-positive foci (data not shown).

3.2. DNA microarray analysis of gene expression

We prepared biotinylated target RNA from GST-P-positive foci and normal liver sections in three hyperplastic nodule-induced rats and three control rats, respectively. Each target was individually hybridized with the Rat 230A Array containing the primary probe sets against well-annotated full-length genes. The scatter plot of the gene expression pattern between three independent control rats showed excellent reproducibility of results with an average correlation coefficient ± S.D. (0.93 ± 0.035). In the case of GST-P-positive foci, good reproducibility was also obtained (average of correlation coefficient ± S.D., 0.95 ± 0.0068). On the other hand, the average of the correlation coefficient ± S.D. derived from comparisons of control versus GST-P-positive foci was 0.74 ± 0.026. These results indicate that expression profiles in the same groups were indistinguishable, but dysregulation in many genes was observed during hepatocarcinogenesis.

3.3. Expression profile of enzymes involved in metabolism and detoxification

Genes were examined in which the expression was enhanced or reduced in GST-P-positive foci compared with control liver. Significantly changed transcripts were selected by moderated t-statistics. There were 15,923 probes on the chip, and 375 and 199 genes were significantly up- and down-regulated, respectively, with log ratio values outside of 1 to −1 ($p < 0.05$). Of these, the twenty most up- and down-regulated genes are shown in Tables 1 and 2 together with p-values for statistical significance. Significant up-regulation of the GST-P gene (*Gstp1/Gstp2*) expression was observed in GST-P-positive foci (Table 1). It is known that enzymes involved in metabolism and detoxification are induced or repressed during chemical hepatocarcinogenesis (Sato, 1989; Suzuki et al., 2004). Overexpression of metabolic enzymes, which were reported to demonstrate increased expression in hyperplastic nodules, including aldehyde dehydrogenase, aflatoxin B1 aldehyde reductase, NAD(P)H dehydrogenase and glutathione peroxidase 2, and the suppression of carbonic anhydrase 3, were detected by DNA microarray analysis (Tables 1 and 2). Semi-quantitative reverse transcriptase-coupled PCR experiments were performed on several selected genes and it was confirmed that the expression patterns were similar to those observed with microarray (data not shown). These results indicate that our study would be suitable for discovering new genes to provide new information on hepatocarcinogenesis, detoxification, and hepatotoxicity.

3.4. Expression profile of transcripts involved in transcription

Probes on the chip were divided into various categories based on Gene Ontology (Ashburner et al., 2000). Observation and analysis of the expression profile for genes involved in transcription, one of the categories, provides valuable information to understand the mechanism of carcinogenesis. Transcripts categorized as transcription with significantly changed expression with log ratio values outside 1 to −1 are listed in Tables 3 and 4, and most have not previously been found to be differentially expressed during chemically induced hepatocarcinogenesis. For example, Pawr was overexpressed in GST-P-positive foci. Pawr also termed par-4, which interacts with Wilms' tumor 1 (WT1) and modulates functions of WT1 (Johnstone et al., 1996). WT1 is a sequence-specific DNA-binding protein and functions as both a tumor suppressor and an oncogenic factor (Loeb and Sukumar, 2002). The WT1 gene exerts an oncogenic function rather than a tumor-suppressor gene function in solid tumors as well as leukemias (Sugiyama, 2001). In prostate cancer cell line, ectopic expression PAWR repressed Bcl-2 expression through WT1 (Cheema et al., 2003). However, Loeb revealed that

Table 1
A list of the twenty genes most highly induced in GST-P-positive foci

Gene symbol	Gene title	Log ratio	*p*-value	GenBank accession no.
Akr1b8	Aldo-keto reductase family 1, member B8	6.65	8.40E−07	NM_173136
Yc2	Glutathione-*S*-transferase Yc2 subunit	5.38	1.32E−06	NM_001009920
Gstp1/Gstp2	Glutathione-*S*-transferase, pi 1/2	5.14	4.31E−06	NM_012577 NM_138974
Aldh1a1	Aldehyde dehydrogenase family 1, member A1	4.42	9.18E−05	NM_022407
Akr7a3	Aflatoxin B1 aldehyde reductase	4.17	4.17E−05	NM_013215
Aldh3a1	Aldehyde dehydrogenase family 3, member A1	3.89	1.07E−04	NM_031972
Nqo1	NAD(P)H dehydrogenase, quinone 1	3.72	9.79E−05	NM_017000
Serpinb 1 a_predicted	Serine (or cysteine) proteinase inhibitor, clade B, member 1a (predicted)	3.72	3.22E−02	NM_001031642
LOC294067	Similar to ww domain binding protein 5	3.71	1.92E−05	XM_215278
RDG:621458	Neurofilament, light polypeptide	3.64	8.68E−04	NM_031783
RGD1310542_predicted	Similar to RIKEN cDNA 4930457P18 (predicted)	3.59	3.13E−04	NM_001014154
–	Brain expressed X-linked 1	3.56	6.18E−04	NM_001037365
Rnf30_predicted	RING finger protein 30 (predicted)	3.54	2.56E−04	NM_001013217
Anxa2	Annexin A2	3.53	6.18E−04	NM_019905
Ca2	Carbonic anhydrase 2	3.51	4.17E−05	NM_019291
Ddit4l	DNA-damage-inducible transcript 4-like	3.45	5.30E−06	NM_080399
Gpx2	Glutathione peroxidase 2	3.41	8.23E−05	NM_183403
RGD:1303152	Ectodermal-neural cortex 1	3.31	1.36E−04	NM_001003401
Dscr1l1	Down syndrome critical region gene 1 -like 1	3.27	3.17E−05	NM_175578
LOC500040	Similar to testis-derived transcript	3.23	2.40E−04	XM_575396

Log ratio indicates a logarithm of the fold-change vs. the expression level of the control rats. Statistics of differential expression between genes was estimated using the linear modeling features of the limma library of the R. Limma computes *p*-values of moderated *t*-statistics by emprical Bayes shrinkage of the standard error toward a common value.

Table 2
A list of the twenty genes most highly repressed in GST-P-positive foci

Gene symbol	Gene title	Log ratio	*p*-value	GenBank accession no.
Pgcl4	Alpha-2u globulin PGCL4	−4.75	1.88E−02	NM_147215
Pgcl3/5/1/4	Alpha-2u globulin PGCL3/5/1/4	−4.71	1.79E−02	NM_147212 NM_147213 NM_147214 NM_147215
Pgcl4	Alpha-2u globulin PGCL4	−4.48	8.86E−03	NM_147215
Ca3	Carbonic anhydrase 3	−3.72	2.20E−02	NM_019292
Apoa4	Apolipoprotein A-IV	−3.63	1.01E−04	NM_012737
Cyp3a13	Cytochrome P450, family 3, subfamily a, polypeptide 13	−3.53	6.18E−04	NP_671739.1
Cyp2c	Cytochrome P450, subfamily IIC (mephenytoin 4-hydroxylase)	−3.50	8.20E−03	NM_019184
Ca3	Carbonic anhydrase 3	−3.45	6.62E−03	NM_019292
LOC368066	Similar to thioether S-methyltransferase	−3.25	2.21E−03	XM_347233
Fasn	Fatty acid synthase	−3.04	2.66E−03	NM_017332
Cyp2a2	Cytochrome P450, subfamily 2A, polypeptide 1	−3.03	2.28E−02	NM_012693
Sult1a2	Sulfotransferase family 1 A, member 2	−2.83	2.52E−03	NM_031732
Ust5r	integral membrane transport protein UST5r	−2.75	2.21E−02	NM_134380
Apoa2	Apolipoprotein A-II	−2.74	1.83E−03	NM_013112
Slc27a5	bile acid CoA ligase	−2.69	2.10E−03	NM_024143
–	Ab2-060	−2.68	1.36E−04	AI411138
Avpr1a	Arginine vasopressin receptor 1A	−2.53	7.61E−03	NM_053019
–	Malic enzyme 3, NADP(+)-dependent, mitochondrial (predicted)	−2.51	6.18E−04	AA964869
Thrsp	Thyroid hormone responsive protein	−2.46	2.54E−04	NM_012703
Slc21a10	Solute carrier family 21, member 10	−2.41	3.05E−02	NM_031650

Log ratio and *p*-value are described in Table 1.

Table 3
A list of genes involved in transcription induced in GST-P-positive foci

Gene Symbol	Gene title	Log ratio	*p*-value	GenBank accession no.
Rnf30_predicted	Ring finger protein 30 (predicted)	3.54	2.56E−04	NM_001013217
Copeb	Core promoter element binding protein	1.92	2.21E−02	NM_031642
Basp1	Brain acidic membrane protein	1.69	1.50E−02	NM_022300
Copeb	Core promoter element binding protein	1.66	1.70E−03	NM_031642
Htatip2_predicted	HIV-1 Tat interactive protein 2 (predicted)	1.61	6.54E−04	XM_214927
L3mbtl2_predicted	l(3)mbt-like 2 (Drosophila) (predicted)	1.59	1.29E−03	NM_001033695
Ppp2ca	Protein phosphatase 2a, catalytic subunit, alpha isoform	1.58	3.77E−03	NM_017039
Ppp2ca	Protein phosphatase 2a, catalytic subunit, alpha isoform	1.56	2.53E−03	AI009467
Maged1	Melanoma antigen, family D, 1	1.41	9.41E−03	NM_053409
Als2cr3	Amyotrophic lateral sclerosis 2 (juvenile) chromosome region, candidate 3 homolog (human)	1.41	4.83E−02	NM_133560
Hmgb2	High mobility group box 2	1.35	4.16E−02	XM_573272
Npm1	Nucleophosmin 1	1.34	4.18E−02	NM_012992
Pdlim1	PDZ and LIM domain 1	1.27	1.22E−02	NM_017365
Mdm2_predicted	Transformed mouse 3T3 cell double minute 2 (predicted)	1.24	2.64E−02	XM_235169
Sox4_predicted	SRY-box containing gene 4 (predicted)	1.19	2.36E−02	XM_344594
Npm1	Nucleophosmin 1	1.18	3.92E−03	NM_012992
Carm1_predicted	Coactivator-associated arginine methyltrnsferase1 (predicted)	1.14	2.07E−02	NM_001030041
Tgif_predicted	TG interacting factor predicted	1.14	3.74E−03	NM_001015020
Ivns 1 abp_predicted	Influenza virus NS1A binding protein (predicted)	1.09	1.09E−02	XM_213898
Pawr	PRKC, apoptosis, WT1, regulator	1.07	4.28E−03	NM_033485
RGD1304726_predicted	Similar to RIKEN cDNA 6330509G02 (predicted)	1.06	2.49E−02	NM_001024993
Ets2	v-ets erythroblastosis virus E26 oncogene homolog 2 (avian)	1.03	1.24E−02	XM_239510
Rbbp7	Retinoblastoma binding protein 7	1.02	4.15E−03	NM_031816

Log ratio and *p*-value are described in Table 1.

WT1 transcriptionally up-regulates anti-apoptotic genes such as Bcl-2 in rhadoid cell line (Loeb, 2006; Mayo et al., 1999). In GST-P-positive foci, we found mRNA overexpression of Bcl-2 (log ratio, 0.776; $p = 0.0330$) by microarray. The different regulation mechanism of Bcl-2 expression is caused by cell lineage and isoform-specific differences in WT1 function (Loeb, 2006; Mayo et al., 1999). Further characterization of Pawr would lead the

Table 4
A list of genes involved in transcription repressed in GST-P-positive foci

Gene symbol	Gene title	Log ratio	*p*-value	GenBank accession no.
Thrsp	Thyroid hormone responsive protein	−2.46	2.54E−04	NM_012703
Thrsp	Thyroid hormone responsive protein	−1.82	2.14E−02	NM_012703
Thrsp	Thyroid hormone responsive protein	−1.68	6.14E−03	NM_012703
Srebf1	Sterol regulatory element binding factor 1	−1.57	4.24E−03	XM_213329
Atf5	Activating transcription factor 5	−1.39	8.82E−03	NM_172336
Sec 14l2	SEC14-like 2 (S. cerevisiae)	−1.36	5.06E−03	NM_053801
	Protocadherin 1 (cadherin-like 1) (predicted)	−1.27	8.40E−03	XM_225997
Gls2	Liver mitochondrial glutaminase	−1.22	1.40E−02	NM_138904
Per2	Period homolog 2	−1.14	7.45E−03	NM_031678
Idb4	Inhibitor of DNA binding 4	−1.12	9.70E−03	NM_175582
Clp1	Cardiac lineage protein 1	−1.11	3.12E−02	NM_001025136
Tgfb1i4	Transforming growth factor beta 1 induced transcript 4	−1.10	5.86E−03	L25785
Rxra	Retinoid X receptor alpha	−1.02	1.24E−03	NM_012805
Hes6_predicted	Hairy and enhancer of split 6 (Drosophila) (predicted)	−1.01	5.41E−03	NM_001013179

Log ratio and *p*-value are described in Table 1.

understanding of oncogenic or tumor suppressor gene function of WT1 during hepatocarcinogenesis.

On the other hand, several sequence-specific DNA-binding transcription factors were repressed during hepatocarcinogenesis (e.g. Sterol-regulatory-element binding factor 1 (Srebf1)/Sterol-regulatory-element binding protein 1 (Srebp1) and retinoid X receptor alpha (RXRalpha)) (Table 4). SREBPs have been established as lipid synthetic transcription factors for cholesterol and fatty acid synthesis (Eberle et al., 2004). The expression of fatty acid synthase and apolipoprotein A-II are mainly regulated by SREBP1, and these genes were suppressed in GST-P-positive foci (Table 2). Further, SREBP1 is required for the induction of thyroid hormone-responsive protein (THRSP) in hepatocytes (Martel et al., 2006). Brown et al. (1997) reported that exposure of Thrsp antisense oligonucleotide inhibited the expression of mRNAs encoding lipogenic (fatty acid synthase, ATP citrate lyase and malic enzyme) and glycolytic (pyruvate kinase) enzymes. The log ratios of these genes were −3.04 ($p = 0.00266$), −1.51 ($p = 0.00105$), −0.508 ($p = 0.0221$) and −2.05 ($p = 0.000531$), respectively. These observations suggest that the aberrant decrease of lipogenic and glycolytic enzymes may be caused by the suppression of SREBP1. This raises the possibility that hepatotoxicity induced by nitroso compounds would be cased by the down regulation of SREBP1.

One of nuclear receptors, retinoid X receptor alpha (RXRalpha) was also decreased in GST-P-positive foci. RXRalpha dimerizes with constitutive androstane receptor (CAR), pregnane X receptor (PXR) and peroxisome proliferator-activated receptor (PPARalpha). Hepatocyte RXRalpha-deficient mice revealed that hepatocyte RXRalpha is required for induction of metabolic enzymes by the ligands of CAR, PXR, and PPARalpha, and is essential for xenobiotic metabolism in vivo (Cai et al., 2002). Hepatotoxicity may be caused by decrease of RXRalpha expression in GST-P-positive foci.

3.5. Expression of transcripts coding chromatin modification enzymes

Sequence-specific transcription factors require cofactors for transcription from the chromatin context and chromatin components affect gene expression (Sterner and Berger, 2000). The expression of cofactors and chromatin components during hepatocarcinogenesis has not been studied well. Recent studies demonstrated that cofactors possess histone modification activities, which are required for the change of chromatin conformation and the regulation of gene function. Generally, histone acetylation promotes transcription, although histone methylation both positively and negatively regulates gene expression dependent on the position of the lysine residue on histone. An epigenetic program including histone and DNA modifications is important for the maintenance of inheritable information and the disturbance of epigenetic balances may lead to alterations in gene expression, resulting in cellular transformation and malignant growth (Lund and van Lohuizen, 2004). Microarray analysis revealed that coactivator-associated arginine methyltransferase (Carm1) and Rbbp7, also termed retinoblastoma suppressor-associated protein 46 (RbAp46), were induced in GST-P-positive foci. CARM1 catalyzes the methylation of histone H3 at Arg17 and can also function as a coactivator for transcription factor NF-E2-related factor 2 (Nrf2), which regulates the induction of Phase II detoxifying enzymes, including GST-P, through its transactivation domain (Lin et al., 2006; Miao et al., 2006). Although increased Nrf2 was detected in hyperplasic nodules, the extremely high level of GST-P expression during hepatocarcinogenesis was difficult to explain by the slight induction of Nrf2 alone (Ikeda et al., 2004). Here we found the overexpression of Carm1 in GST-P-positive foci. Increase of both Nrf2 and Carm1 expression and the cooperative regulation of gene expression may lead to the induction of GST-P expression during hepatocarcinogenesis.

We also found the induction of RbAp46, which contributed to the regulation of gene expression as a subunit of histone acetyltransferase, histone deacetylase and chromatin remodeling complexes NURD (Zhang et al., 1999). Li et al., 2003 reported that the expression of RbAp46 suppressed colony formation in soft agar, and inhibited tumor formation in nude mice. They also showed that high levels of RbAp46 expression promoted apoptotic cell death, resulting in the inhibition of tumorigenicity of neoplastigenic breast epithelial cells. These results suggest that overexpressed RbAp46 in GST-P-positive cells may function as a suppressor of tumorigenicity in the early stage of hepatocarcinogenesis.

3.6. Expression of transcripts coding chromatin components and related factors

High mobility group box 2 (Hmgb2), a member of HMGB family proteins, was up-regulated in GST-P-positive cells. HMGB proteins are abundant nonhistone nuclear proteins that have been found in association with chromatin. HMGB family proteins contain two DNA-binding HMG-box domains and bind to DNA without sequence specificity, but play important architectural roles in the assembly of nucleoprotein complexes in a variety of biological processes including the initiation

of transcription and DNA repair (Thomas, 2001). Further, HMGB2, while showing no coactivator activity on its own, can promote transcription activity together with histone acetyltransferase. HMGB2 acts mainly at the level of elongation and is a coactivator for transcription from chromatin templates (Guermah et al., 2006). Hmgb2 is frequently overexpressed in malignant gastrointestinal stromal tumors and ovarian cancer (Koon et al., 2004; Ouellet et al., 2006). Overexpression of Hmgb2 may be common feature of carcinogenesis. HMGB2 binds with high affinity to DNA modified with the cancer chemotherapeutic drug cisplatin and enhancement of cisplatin sensitivity in Hmgb2 transfected human lung cancer cells (Arioka et al., 1999; Farid et al., 1996). Cisplatin-induced hepatotoxicity may be promoted by overexpressed Hmgb2.

Nucleophosmin was identified as a positively regulated gene in GST-P-positive cells. Nucleophosmin is a key regulator for centrosome duplication, the maintenance of genomic integrity, and ribosome assembly. At the steady state, nucleophosmin localizes mainly in the nucleolus, whereas aberrant cytoplasmic localization of nucleophosmin is observed in acute myeloid leukemias (Mariano et al., 2006). Observation of localization of nucleophosmin would be important for the understanding of roles of overexpressed nucleophosmin in GST-P-positive foci. Recent studies suggest that nucleophosmin may be a Ran-Crm1 substrate that controls centrosome duplication and utilizes a conserved Crm1-dependent nuclear export sequence in its amino terminus to enable shuttling between the nucleolus/nucleus and cytoplasm (Wang et al., 2005; Yu et al., 2006). Further, purification of nucleophosmin binding protein revealed that nucleophosmin directly interacted with ribosomal protein L5. This interaction mediated the colocalization of nucleophosmin with both maturing nuclear 60S ribosomal subunits and newly exported and assembled 80S ribosomes (Yu et al., 2006). Interestingly, Crm1 (log ratio, 0.908; $p = 0.0427$) and ribosomal protein L5 (log ratio, 0.830; $p = 0.00429$) were also up-regulated in GST-P-positive foci. Overexpression of these genes may disturb multiple processes involved in nucleophosmin, which accelerate oncogenesis.

DNA microarray analysis in this study uncovered several genes, which expression was induced or repressed during hepatocarcinogenesis, and some of these genes possess anti-oncogenic as well as oncogenic activities and may be involved in regulation of GST-P expression. Our study provided a candidate gene link to the early stage of carcinogenesis and hepatotoxicity. To elucidate the mechanisms of the early stage of hepatocarcinogenesis mediated by these genes, further characterization of aberrantly expressed genes in GST-P-positive cells is necessary. We proceed to observe the effect of overexpression of these genes up-regulated during hepatocarcinogenesis, especially epigenetics regulatory factors, on transformation and the induction of GST-P expression.

Acknowledgements

This research was supported in part by grants from the Ministry of Education, Culture, Sports, Science and Technology (MEXT), Japan, Japan Society for the Promotion of Science (JSPS), a Grant-in-Aid for Scientific Research from the Ministry of Health and Labor of Japan, Long-range Research Initiative (LRI) by Japan Chemical Industry Association (JCIA) and Sankyo Foundation of Life Science.

References

Arioka, H., Nishio, K., Ishida, T., Fukumoto, H., Fukuoka, K., Nomoto, T., Kurokawa, H., Yokote, H., Abe, S., Saijo, N., 1999. Enhancement of cisplatin sensitivity in high mobility group 2 cDNA-transfected human lung cancer cells. Jpn. J. Cancer Res. 90, 108–115.

Ashburner, M., Ball, C.A., Blake, J.A., Botstein, D., Butler, H., Cherry, J.M., Davis, A.P., Dolinski, K., Dwight, S.S., Eppig, J.T., Harris, M.A., Hill, D.P., Issel-Tarver, L., Kasarskis, A., Lewis, S., Matese, J.C., Richardson, J.E., Ringwald, M., Rubin, G.M., Sherlock, G., 2000. Gene ontology: tool for the unification of biology. The Gene Ontology Consortium. Nat. Genet. 25, 25–29.

Brown, S.B., Maloney, M., Kinlaw, W.B., 1997. "Spot 14" protein functions at the pretranslational level in the regulation of hepatic metabolism by thyroid hormone and glucose. J. Biol. Chem. 272, 2163–2166.

Cai, Y., Konishi, T., Han, G., Campwala, K.H., French, S.W., Wan, Y.J., 2002. The role of hepatocyte RXR alpha in xenobiotic-sensing nuclear receptor-mediated pathways. Eur. J. Pharm. Sci. 15, 89–96.

Cheema, S.K., Mishra, S.K., Rangnekar, V.M., Tari, A.M., Kumar, R., Lopez-Berestein, G., 2003. Par-4 transcriptionally regulates Bcl-2 through a WT1-binding site on the bcl-2 promoter. J. Biol. Chem. 278, 19995–20005.

Eberle, D., Hegarty, B., Bossard, P., Ferre, P., Foufelle, F., 2004. SREBP transcription factors: master regulators of lipid homeostasis. Biochimie 86, 839–848.

Eriksson, L.C., Sharma, R.N., Roomi, M.W., Ho, R.K., Farber, E., Murray, R.K., 1983. A characteristic electrophoretic pattern of cytosolic polypeptides from hepatocyte nodules generated during liver carcinogenesis in several models. Biochem. Biophys. Res. Commun. 117, 740–745.

Farid, R.S., Bianchi, M.E., Falciola, L., Engelsberg, B.N., Billings, P.C., 1996. Differential binding of HMG1, HMG2, and a single HMG box to cisplatin-damaged DNA. Toxicol. Appl. Pharmacol. 141, 532–539.

Guermah, M., Palhan, V.B., Tackett, A.J., Chait, B.T., Roeder, R.G., 2006. Synergistic functions of SII and p300 in productive activator-dependent transcription of chromatin templates. Cell 125, 275–286.

Ikeda, H., Nishi, S., Sakai, M., 2004. Transcription factor Nrf2/MafK regulates rat placental glutathione-*S*-transferase gene during hepatocarcinogenesis. Biochem. J. 380, 515–521.

Ito, N., Tamano, S., Shirai, T., 2003. A medium-term rat liver bioassay for rapid in vivo detection of carcinogenic potential of chemicals. Cancer Sci. 94, 3–8.

Johnstone, R.W., See, R.H., Sells, S.F., Wang, J., Muthukkumar, S., Englert, C., Haber, D.A., Licht, J.D., Sugrue, S.P., Roberts, T., Rangnekar, V.M., Shi, Y., 1996. A novel repressor, par-4, modulates transcription and growth suppression functions of the Wilms' tumor suppressor WT1. Mol. Cell. Biol. 16, 6945–6956.

Koon, N., Schneider-Stock, R., Sarlomo-Rikala, M., Lasota, J., Smolkin, M., Petroni, G., Zaika, A., Boltze, C., Meyer, F., Andersson, L., Knuutila, S., Miettinen, M., El-Rifai, W., 2004. Molecular targets for tumour progression in gastrointestinal stromal tumours. Gut 53, 235–240.

Li, G.C., Guan, L.S., Wang, Z.Y., 2003. Overexpression of RbAp46 facilitates stress-induced apoptosis and suppresses tumorigenicity of neoplastigenic breast epithelial cells. Int. J. Cancer 105, 762–768.

Lin, W., Shen, G., Yuan, X., Jain, M.R., Yu, S., Zhang, A., Chen, J.D., Kong, A.N., 2006. Regulation of Nrf2 transactivation domain activity by p160 RAC3/SRC3 and other nuclear co-regulators. J. Biochem. Mol. Biol. 39, 304–310.

Loeb, D.M., 2006. WT1 Influences apoptosis through transcriptional regulation of Bcl-2 family members. Cell Cycle 5, 1249–1253.

Loeb, D.M., Sukumar, S., 2002. The role of WT1 in oncogenesis: tumor suppressor or oncogene? Int. J. Hematol. 76, 117–126.

Lund, A.H., van Lohuizen, M., 2004. Epigenetics and cancer. Genes Dev. 18, 2315–2335.

Mariano, A.R., Colombo, E., Luzi, L., Martinelli, P., Volorio, S., Bernard, L., Meani, N., Bergomas, R., Alcalay, M., Pelicci, P.G., 2006. Cytoplasmic localization of NPM in myeloid leukemias is dictated by gain-of-function mutations that create a functional nuclear export signal. Oncogene 25, 4376–4380.

Martel, P.M., Bingham, C.M., McGraw, C.J., Baker, C.L., Morganelli, P.M., Meng, M.L., Armstrong, J.M., Moncur, J.T., Kinlaw, W.B., 2006. S14 protein in breast cancer cells: direct evidence of regulation by SREBP-1c, superinduction with progestin, and effects on cell growth. Exp. Cell Res. 312, 278–288.

Mayo, M.W., Wang, C.Y., Drouin, S.S., Madrid, L.V., Marshall, A.F., Reed, J.C., Weissman, B.E., Baldwin, A.S., 1999. WT1 modulates apoptosis by transcriptionally upregulating the bcl-2 proto-oncogene. EMBO J. 18, 3990–4003.

Miao, F., Li, S., Chavez, V., Lanting, L., Natarajan, R., 2006. Coactivator-associated arginine methyltransferase-1 enhances nuclear factor-kappaB-mediated gene transcription through methylation of histone H3 at arginine 17. Mol. Endocrinol. 20, 1562–1573.

Morimura, S., Suzuki, T., Hochi, S., Yuki, A., Nomura, K., Kitagawa, T., Nagatsu, I., Imagawa, M., Muramatsu, M., 1993. Transactivation of glutathione transferase P gene during chemical hepatocarcinogenesis of the rat. Proc. Natl. Acad. Sci. U.S.A. 90, 2065–2068.

Ouellet, V., Page, C.L., Guyot, M.C., Lussier, C., Tonin, P.N., Provencher, D.M., Mes-Masson, A.M., 2006. SET complex in serous epithelial ovarian cancer. Int. J. Cancer 119, 2119–2126.

Sakai, M., Muramatsu, M., 2005. Regulation of GST-P gene expression during hepatocarcinogenesis. Methods Enzymol. 401, 42–61.

Sato, K., 1989. Glutathione transferase as markers of preneoplasia and neoplasia. Adv. Cancer Res. 52, 205–255.

Satoh, K., Hatayama, I., Tateoka, N., Tamai, K., Shimizu, T., Tatematsu, M., Ito, N., Sato, K., 1989. Transient induction of single GST-P positive hepatocytes by DEN. Carcinogenesis 10, 2107–2111.

Satoh, K., Kitahara, A., Soma, Y., Inaba, Y., Hatayama, I., Sato, K., 1985. Purification, induction, and distribution of placental glutathione transferase: a new marker enzyme for preneoplastic cells in the rat chemical hepatocarcinogenesis. Proc. Natl. Acad. Sci. U.S.A. 82, 3964–3968.

Satoh, K., Takahashi, G., Miura, T., Hayakari, M., Hatayama, I., 2005. Enzymatic detection of precursor cell populations of preneoplastic foci positive for gamma-glutamyltranspeptidase in rat liver. Int. J. Cancer 115, 711–716.

Solt, D., Farber, E., 1976. New principle for the analysis of chemical carcinogenesis. Nature 263, 701–703.

Sterner, D.E., Berger, S.L., 2000. Acetylation of histones and transcription-related factors. Microbiol. Mol. Biol. Rev. 64, 435–459.

Sugiyama, H., 2001. Wilms' tumor gene WT1: its oncogenic function and clinical application. Int. J. Hematol. 73, 177–187.

Suzuki, S., Asamoto, M., Tsujimura, K., Shirai, T., 2004. Specific differences in gene expression profile revealed by cDNA microarray analysis of glutathione-*S*-transferase placental form (GST-P) immunohistochemically positive rat liver foci and surrounding tissue. Carcinogenesis 25, 439–443.

Suzuki, T., Imagawa, M., Hirabayashi, M., Yuki, A., Hisatake, K., Nomura, K., Kitagawa, T., Muramatsu, M., 1995. Identification of an enhancer responsible for tumor marker gene expression by means of transgenic rats. Cancer Res. 55, 2651–2655.

Thomas, J.O., 2001. HMG1 and 2: architectural DNA-binding proteins. Biochem. Soc. Trans. 29, 395–401.

Wang, W., Budhu, A., Forgues, M., Wang, X.W., 2005. Temporal and spatial control of nucleophosmin by the Ran-Crm1 complex in centrosome duplication. Nat. Cell Biol. 7, 823–830.

Yu, Y., Maggi Jr., L.B., Brady, S.N., Apicelli, A.J., Dai, M.S., Lu, H., Weber, J.D., 2006. Nucleophosmin is essential for ribosomal protein L5 nuclear export. Mol. Cell. Biol. 26, 3798–3809.

Zhang, Y., Ng, H.H., Erdjument-Bromage, H., Tempst, P., Bird, A., Reinberg, D., 1999. Analysis of the NuRD subunits reveals a histone deacetylase core complex and a connection with DNA methylation. Genes Dev. 13, 1924–1935.

J Pharmacol Sci 101, 267 – 270 (2006)

Journal of Pharmacological Sciences

Current Perspective

MicroRNA: Biogenetic and Functional Mechanisms and Involvements in Cell Differentiation and Cancer

Soken Tsuchiya[1], Yasushi Okuno[1], and Gozoh Tsujimoto[1,*]

[1]*Department of Genomic Drug Discovery Science, Graduate School of Pharmaceutical Sciences, Kyoto University, 46-29 Yoshida Shimoadachi-cho, Sakyo-ku, Kyoto 606-8501, Japan*

Received June 2, 2006

Abstract. MicroRNAs (miRNAs) are endogenous small noncoding RNAs (20 – 23 nucleotides) that negatively regulate the gene expressions at the posttranscriptional level by base pairing to the 3' untranslated region of target messenger RNAs. Hundreds of miRNAs have been identified in humans and evolutionarily conserved from plants to animals. It is revealed that miRNAs regulate various physiological and pathological pathways such as cell differentiation, cell proliferation, and tumoriogenesis. By the computational analysis, it is predicted that 30% of protein-encoding genes are regulated by miRNAs. In this review, we discuss recent remarkable advances in the miRNA biogenetic and functional mechanisms and the involvements of miRNAs in cell differentiation, especially in hematopoietic lineages, and cancer. These evidences offer the possibility that miRNAs would be potentially useful for drug discovery.

Keywords: microRNA, RNA cleavage, translational repression, target mRNA, base pairing

Introduction

MicroRNAs (miRNAs) are endogenous short non-coding RNA molecules (20 – 23 nucleotides) that regulate cell differentiation, cell proliferation, and apoptosis through post-transcriptional suppression of gene expression by binding to the complementary sequence in the 3' untranslated region (3'UTR) of target messenger RNAs (mRNAs) (1). Hundreds of miRNAs have been identified in humans and they are evolutionarily conserved (1, 2). In addition, the presence of up to 1000 miRNAs is estimated by computational analysis (3). Strikingly, 30% of protein-encoding genes in humans are predicted to be regulated by miRNAs (4). Recently, it has been revealed that altered expression of specific miRNA genes contributes to the initiation and progression of diseases such as cancer (5 – 10). This review focuses on the biogenetic and functional mechanisms and the involvements in cell differentiation and cancer in mammalian miRNAs and the utility of miRNAs in drug discovery.

*Corresponding author. gtsuji@pharm.kyoto-u.ac.jp
Published online in J-STAGE
doi: 10.1254/jphs.CPJ06013X

Invited article

Mechanisms of biogenesis and function

Most miRNA genes are located in the introns of host genes or outside genes. Unlike *Drosophila*, most of the human miRNA genes individually exist, although some human miRNAs are found in polycistronic clusters (5, 8, 9).

The miRNAs are synthesized through multiple steps (Fig. 1). Initially, the miRNAs are transcribed as long RNA precursors (pri-miRNAs) (11). As pri-miRNAs usually contain the cap structure and the poly(A) tail, it is suggested that the transcription of miRNAs is carried out by RNA polymerase II (12). The pri-miRNAs are processed into the precursors of approximately 70 nucleotides (pre-miRNAs) with a stem-loop structure and a two nucleotide 3' overhang by the RNase III enzyme Drosha and the double-stranded-RNA-binding protein DGCR8/Pasha (13, 14), and pre-miRNAs are exported from the nucleus to the cytoplasm by Exportin-5 in a Ran guanosine triphosphate-dependent manner (15). Pre-miRNAs exported in the cytoplasm are processed by another RNase III enzyme, Dicer, and only one strand (guide strand) as a mature

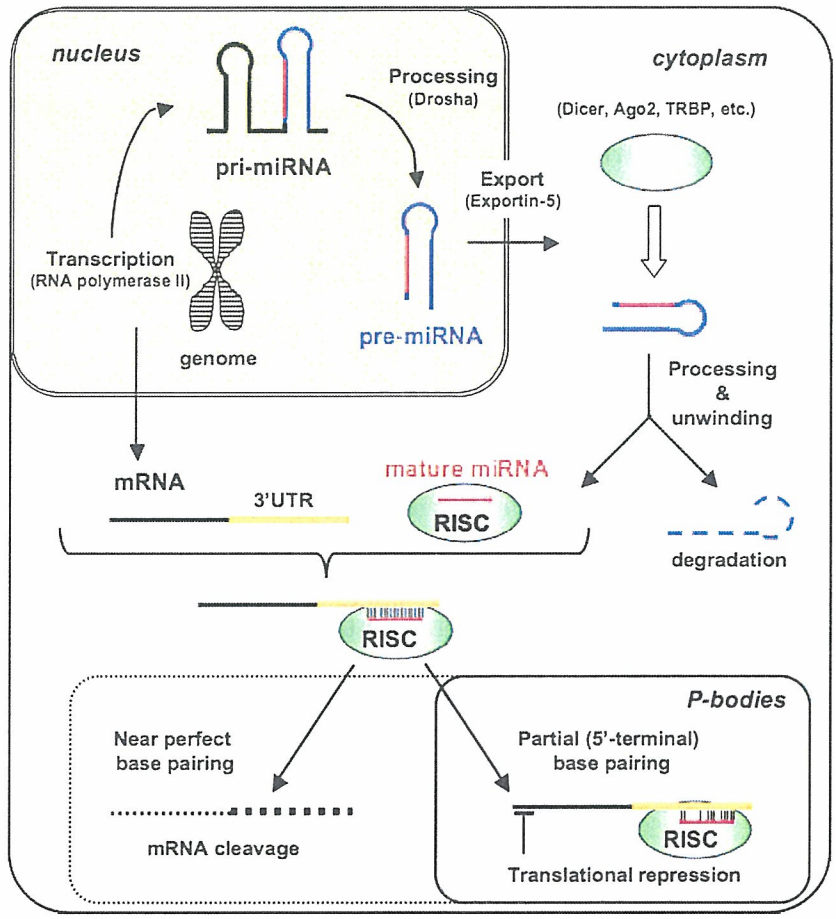

Fig. 1. Diagram of the miRNA biogenetic and functional mechanisms. Whether the target mRNA cleavage by RISC occurs in the cytoplasm or P-bodies remains unknown.

miRNA is incorporated into a RNA-induced silencing complex (RISC) that mediates either target RNA cleavage or translational inhibition, while the another strand (passenger strand) is excluded. Which strand is incorporated in RISC is determined by the stability of the base pairs at the 5' end of the duplex (16, 17). The incorporated guide strand guides the RISC to the complementary sequence in the 3'UTR of target mRNA. When the guide strand shares perfect or near perfect base pairing with the 3'UTR of target mRNA, the target mRNA is degraded by Argonaute2 (Ago2), a component of RISC (18). On the contrary, when the guide strand shares partial base pairing, translation is target-specifically repressed without the target mRNA degradation (19). Recent studies have revealed that RISC is at least composed of Dicer, Ago2, and the double-strand RNA binding protein TRBP, and RISC efficiently processes pre-miRNAs to mature miRNAs (20). Furthermore, RISC more efficiently cleaves target mRNAs by using the pre-miRNAs than the duplex miRNAs that do not have the stem-loop. These results suggest that miRNA processing by Dicer, assembly of the mature miRNA into RISC, and target RNA cleavage by Ago2 are coupled. Compared to the RNA cleavage mechanism by Ago2, the translational repression mechanism by miRNAs had been poorly understood. Recently, it was revealed that the target mRNAs binding to RISC through partial base pairing are accumulated in the cytoplasmic foci referred to as processing bodies (P-bodies) (21, 22). P-bodies, in which the mRNAs are stored or degraded by the decapping enzymes and exonucleases, do not contain the translational machinery (23). Furthermore, the disruption of P-bodies by the silencing of GW182, a key protein in P-body, inhibits translational silencing in not only partial base pairing but also perfect base pairing (24), although the localization of target mRNA with perfect base pairing is not detected in P-bodies (21). These results suggest that, at least in part, translational repression appears to be caused by the recruitment of target mRNAs to P-bodies. However, whether localiza-

tion of the RISC-target mRNA complex in P-bodies is a cause or a result of the translational repression and whether the target mRNA cleavage by RISC occurs in the cytoplasm or P-bodies remain controversial issues.

Cell differentiation

Increasing evidence indicates that miRNAs have distinct expression patterns among tissues and cells in different differentiation stage (25). It is reported that overexpression of miR-124, which is preferentially expressed in brain, shifted the gene expression profile of HeLa cells towards that of the brain. Similarly, overexpression of miR-1 shifted the expression profile towards that of the muscle in that miR-1 is preferentially expressed (25). These results indicate that miRNAs play important roles in cell differentiation and characterization.

Recently, it was revealed that miRNAs also played critical roles in the differentiation of mammalian hematopoietic lineage. For example, miR-181 is preferentially expressed in the thymus and B-lymphoid cells of mouse bone marrow and promotes B cell differentiation by overexpression in hemapoietic stem/progenitor cells (26). Conversely, overexpression of the miR-181a, one member of the miR-181 family, was reported to repress megakaryoblast differentiation in humans (27). By the induction of megakaryoblast differentiation, the expression of endogenous miR-181a is downregulated through the acetylcholinesterase, protein kinase (PK) C, and PKA cascade. The expression of miR-130a is also downregulated by the induction of megakaryoblast differentiation (28). miR-130a targets the transcriptional factor MAFB that is a transcriptional activator of GPIIB, an important protein for platelet physiology. Furthermore, miR-223 is upregulated by the retinoic acid-induced replacement of NFI-A with CCAAT/Enhancer binding protein (C/EBP) α, and promotes human granulopoiesis (29). As miR-223 repressed NFI-A translation, the upregulation of miR-223 by C/EBPα and granulopoiesis further accelerated through positive feedback by miR-223.

Cancer

It has been revealed that the change of miRNA expressions contributes to the initiation and progression of cancer. More than 50% of miRNAs are located in cancer-associated genomic regions or in fragile sites (5). The expression of miR-15a and miR-16, which locate as a cistronic cluster at 13q14, is deleted or decreased in most cases (approx. 68%) of B cell chronic lymphocytic leukemia (B-CLL) (6). Both these miRNAs negatively regulate the expression of B cell lymphoma 2 (Bcl2), that is reported to be expressed in many types of cancer including leukemias, and inhibit cell death (7). Overexpression of miR-15 and miR-16 in the MEG-01 cell line actually induces the apoptosis. Inversely, one cluster of miRNAs, miR-17 – 92 polycistron, was found to increase in the cancers such as B-CLL (8). The expression of six miRNAs in this cluster is upregulated by c-myc, whose expression and/or function are one of the most common abnormalities in human cancers, and miR-17-5p and miR-20a included in this cluster negatively regulate the expression of transcriptional factor E2F1 (9). Furthermore, mice reconstituted with hemotopoietic stem cells overexpressing miR-17 – 19b exhibit accelerated c-myc-induced lymphomagenesis (8). Furthermore, it was revealed that miRNA expression profiles enable researchers to successfully classify poorly characterized human tumors that can not be accurately classified by mRNA expression profiles (10). These results show the possibility that miRNAs have clinical benefits as not only therapeutic targets but also a tool for cancer diagnosis.

Drug discovery

miRNAs are expected to be potential targets of therapeutic strategies applied to drug discovery for a number of reasons. Firstly, in addition to the initiation and progression of tumor, miRNAs play critical roles in various biological pathways such as differentiation of adipocyte and insulin secretion and diseases such as diabetes and hepatitis. Therefore, the possibility that various human diseases are caused by abnormalities in miRNAs is indicated. Actually, miR-15 and miR-16 have been deleted or decreased in most cases of B-CLL and are identified as tumor suppressor genes (6, 7). Secondly, miRNA expression profiles are correlated with clinical severity of cancer malignancy, and because of this, miRNAs are expected to be powerful tools for cancer diagnosis (10). Thirdly, miRNAs are applicable in gene therapy. The expression of miRNAs can be introduced in vivo by using viral vectors and chemical modifications. Finally, antisense oligonucleotides are potent inhibitors of miRNA, and they can be applied to gene therapy. Actually, it was reported that introduction of 2'-*O*-methoxyethyl phosphorothioate antisense oligonucleotide of miR-122, which is abundant in the liver and regulates cholesterol and fatty-acid metabolism, decreases plasma cholesterol levels and improves liver steatosis in mice with diet-induced obesity (30). These findings indicate that miRNAs and the antisense oligonucleotides are potential targets for drug discovery.